JOURNAL OF PETROLOGY | VOLUME 37 | NUMBER 6 | PAGES 1491–1521 | 1996

NICK PETFORD[1] and MICHAEL ATHERTON[2]*

[1]SCHOOL OF GEOLOGICAL SCIENCES, KINGSTON UNIVERSITY, KINGSTON UPON THAMES KT1 2EE, UK

[2]DEPARTMENT OF EARTH SCIENCES, UNIVERSITY OF LIVERPOOL, JANE HERDMAN LABORATORIES, BROWNLOW STREET, LIVERPOOL L69 3BX, UK

Na-rich Partial Melts from Newly Underplated Basaltic Crust: the Cordillera Blanca Batholith, Peru

The late Miocene Cordillera Blanca Batholith lies directly over thick (50 km) crust, inboard of the older Cretaceous Coastal Batholith. Its peraluminous 'S' type mineralogy and its position suggest recycling of continental crust, which is commonly thought to be an increasingly important component in magmas inboard of continental margins. However, the peraluminous, apparent 'S' type character of the batholith is an artefact of deformation and uplift along a major crustal lineament. The batholith is a metaluminous 'I' type and the dominant high-silica rocks (>70%) are Na rich with many of the characteristics of subducted oceanic slab melts. However, the position of the batholith and age of the oceanic crust at the trench during the Miocene preclude slab melting. Instead, partial melting of newly underplated Miocene crust is proposed. In this dynamic model newly underplated basaltic material is melted to produce high-Na, low HREE, high-Al 'trondhjemitic' type melts with residues of garnet, clinopyroxene and amphibole. Such Na-rich magmas are characteristic of thick Andean crust; they are significantly different from typical calc-alkaline, tonalite–granodiorite magmas, and their presence along the spine of the Andes provokes questions about models of trondhjemite genesis by melting of subducted oceanic crust, as well as any generalized, circum-Pacific model involving consistent isotopic or chemical changes inboard from the trench.

KEY WORDS: *batholith; modified 'I' type granite; Na-rich magma; thick crust*

INTRODUCTION

Mesozoic–Tertiary calc-alkaline batholiths constitute a major component of the magmatism of the Andean margin. Although the parent magmas have a substantial mantle component (Miller & Harris, 1989), recycling of crust is to be expected by analogy with the Himalayas, the other active continental margin characterized by very thick crust. In active continental margins there is commonly a switch to 'S' type or crustally derived granites inboard of granites with a mainly mantle signature (Pitcher, 1983). Here we describe the Cordillera Blanca Batholith of Peru. This lies inboard of the Coastal Batholith (Fig. 1), directly over the massively thickened keel of the Andes. Given the unique tectonic position of the Cordillera Blanca as the final component in an easterly younging plutonic sequence intruded into thickened continental crust, recycling of old continental crust might be expected. Reconnaissance studies (Cobbing *et al.*, 1981; Pitcher, 1983) concluded that the peraluminous rocks of the batholith were indeed 'S' type, i.e. derived from a sedimentary source (Chappell & White, 1974). This thinking was partly based on the belief that the Precambrian crystalline Arequipa basement 'is an essential element in Andean structure' (Cobbing, 1985, p. 5) which floors the whole of the Andean margin and was probably the source of the batholith magmas. However, subsequent studies demonstrated that the peraluminous or 'S' type character is confined to rocks of the western deformed margin of the batholith and it was considered by Atherton & Sanderson (1987) to be related to high-level late-stage fluid interaction with the aluminous country rocks into which the batholith was intruded. New major and trace element [including rare earth element (REE)] and Sr, Nd and O isotope data are used to define the geochemical variation within the batholith, to assess the

*Corresponding author.

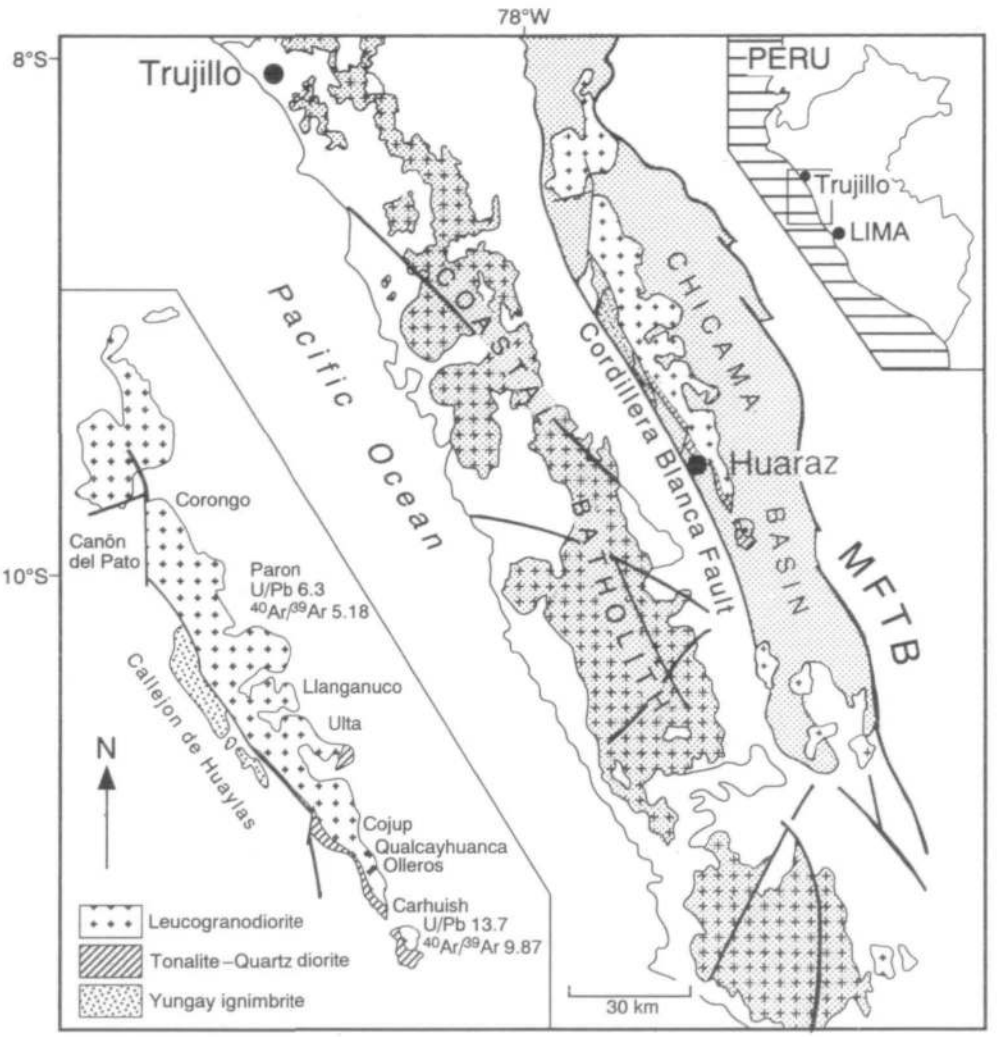

Fig. 1. Simplified map of mid–northern Peru showing the Cordillera Blanca Batholith, bounded to the west by the Cordillera Blanca Fault System and lying within the Jurassic basin fill of the Chicama Formation. The eastern boundary of this basin is marked by the Maranon Thrust and Fold Belt (MTFB), which is also the eastern limit of the west Peruvian Trough of Wilson & Garayar (1967). Inset shows the distribution of leucogranodiorite and tonalite–quartz diorite, and recent U/Pb zircon (Mukasa, 1984) and $^{40}Ar/^{39}Ar$ (Petford & Atherton, 1992) ages. The 5·18 and 6·3 Ma ages are from leucogranodioritic rocks from the Llanganuco traverse, whereas the older ages, including the U/Pb zircon age of 13·7 Ma, are from the early basic facies rocks in the southern Carhuish area.

relative role of crust and mantle components, to relate fluid infiltration to deformation, to determine the relationship between crustal thickening and the origin of the batholith and to determine and explain the compositional changes inboard from the Coastal Batholith.

GEOLOGICAL FRAMEWORK

The Cordillera Blanca Batholith is situated in the high Andes of northwestern Peru between 8 and 10°S. It is >200 km long but may extend even further as it plunges beneath the cover to the south (Fig.1). Radiometric ages indicate a Miocene–Pliocene age of intrusion (Cobbing *et al.*, 1981).

The batholith was intruded into the Chicama Formation, a 2000 m thick basinal sequence of Upper Jurassic shales intercalated with siltstones, quartzite and volcanic rocks (Fig. 1). The rocks were deformed and uplifted in the Eocene, most of the deformation being concentrated to the east in the Maranon Fold and Thrust Belt (MFTB, Mégard, 1989). During the Miocene there were three short periods of compressional activity [Quechua 1–3 of Mégard (1989) at ~20 Ma, 9 Ma and 6–3 Ma] separated by neutral or extensional periods. The

Cordillera Blanca Batholith and coeval ignimbrites (Yungay Formation) intruded and ejected over the period 14–3 Ma represent the final magmatic events in central Peru associated with the extensional periods between the Quechua events (Petford & Atherton, 1992).

The western margin of the batholith is bounded and strongly deformed by the Cordillera Blanca Fault System (Fig. 1), a NNW–SSE-striking normal fault complex extending >200 km in length which is still active (Mégard & Philip, 1976; Sebrier *et al.*, 1988). This fault system is the dominant structure in this part of western Peru (Cobbing *et al.*, 1981), representing a long-lived crustal lineament which marks the western margin of the Jurassic basin, and later, controlled magma ascent, and post-emplacement uplift of the batholith owing to buoyancy forces at high crustal levels (Petford & Atherton, 1992).

The geology of the area was first described by Steinmann (1910) but it was not until 1956 that Egeler & De Booy published the first geological map of an area between 9°20′ and 9°40′S (about a sixth of the batholith) in very high difficult country. More recent reconnaissance studies have provided limited field, chemical and age data (Wilson & Garayer, 1967; Cobbing *et al.*, 1981; Atherton & Sanderson, 1987), and the Miocene and Recent tectonics have been described by French workers (e.g. Sebrier *et al.*, 1988; Mégard, 1989).

THE STRUCTURE OF THE CRUST OF NORTH-CENTRAL PERU

Recently, Fukao *et al.* (1989) published the results of a 4 year gravity survey across the Peruvian Andes, supporting the earlier seismological work of James (1971) which showed that the crust thickens southwards from 45–50 km in Northern Peru to 50–60 km in Central Peru (Fig. 2), reaching a maximum of 70 km beneath the Altiplano. The major thickening is associated with material of density 3·0 g/cm^3 (P-wave velocity of 6·5–7·0 km/s). A detailed gravity survey at latitude 9°S (Couch *et al.*, 1981), also emphasizes the deep crustal keel beneath the Cordillera and a lower and middle crust dominated by 3·0 g/cm^3 material (Fig. 2). These densities are consistent with the presence of a mafic underplate at the base of the crust. Detailed modelling including seismic refraction studies and crustal shortening estimates further south (21–24°S) also indicates that the thickened crust beneath the Western Cordillera

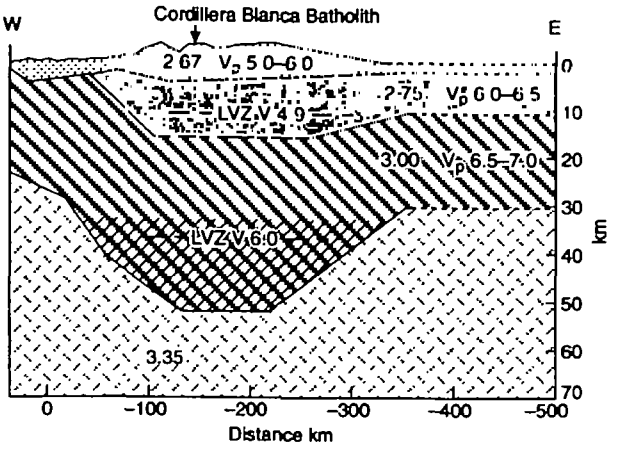

Fig. 2. West–east cross-section through the batholith showing the crustal structure at 9°S, with densities after Couch *et al.* (1981). Corresponding velocity data from Wilson (1985). The low-velocity zones (LVZ) with velocities are from Ocola & Meyer (1972). Lined part of the lower crust is the underplated keel.

probably results from magma addition from the asthenospheric wedge (Schmitz, 1994).

At present, the Nazca plate is subducting beneath the Peruvian Andes at a velocity of 10 mm/yr, and the dip of the slab is 30° just off the coast, then it follows a quasi-horizontal trajectory inland (Suarez *et al.*, 1983). Subduction angles during the Miocene are thought to have been similar to those today (see Kono *et al.*, 1989). Fukao *et al.* (1989), using a three-layer gravity crustal model and earthquake foci, showed that there is a clear mantle wedge under the Cordillera Blanca which is absent further south owing to subduction of the buoyant Nazca ridge.

STRUCTURE OF THE BATHOLITH

Details of the structure of the Cordillera Blanca Batholith and the mode of intrusion have been given by Petford & Atherton (1992) and only a short synopsis is given here to facilitate relation of the different granite types to deformation. Strong deformation is confined to the western margin and is clearly fault related, occurring during and after batholith emplacement. Pre-full crystallization, high melt-fraction fabrics, including biotite schlieren, layering and aggregates of magmatic phenocrysts, are confined to the undeformed core of the batholith. These pass into low-melt fraction–metamorphic fabrics and ultimately late brittle and cataclastic structures at the intensely deformed western margin (see Petford & Atherton, 1992). The westward intensification of the deformation fabric

culminates in ribbon quartz in the plane of the mica foliation. Such textures only occur when the host rock is in the solid state and reflect high shear strains associated with late uplift. Regional structures indicate a dominantly tensional stress regime during the Oligo-Miocene in the Western Cordillera, which, on the basis of the neotectonic structures, is still undergoing extensional collapse (Sebrier *et al.*, 1988).

THE MAIN FACIES AND MINERALOGY OF THE BATHOLITH

The major mineral phases are plagioclase, K-feldspar, quartz, amphibole and/or biotite (Egeler & De Booy, 1956; Atherton & Sanderson, 1987) with individual rocks ranging from quartz diorite–monzonite to evolved granite (Fig. 3). The rocks as a whole define a crude calc-alkaline trend (Lameyre & Bowden, 1982) on a QAP plot (Fig. 3). Detailed mapping in a small area in the south of the batholith by Egeler & De Booy (1956) defined three major units: (1) leucogranodiorite (>70% SiO_2); (2) granodiorite; (3) tonalite–quartz monzodiorite. Leucogranodiorite dominates (>85% of the batholith), and the other units form older subordinate–discrete outcrops occurring mainly in the south and at the margins of the batholith (Fig. 1). Although the field definitions of Egeler & De Booy (1956) are not entirely consistent with the QAP nomenclature, we have retained the general three-fold division, as the rock units they recognized in the field appear to be represented throughout the batholith.

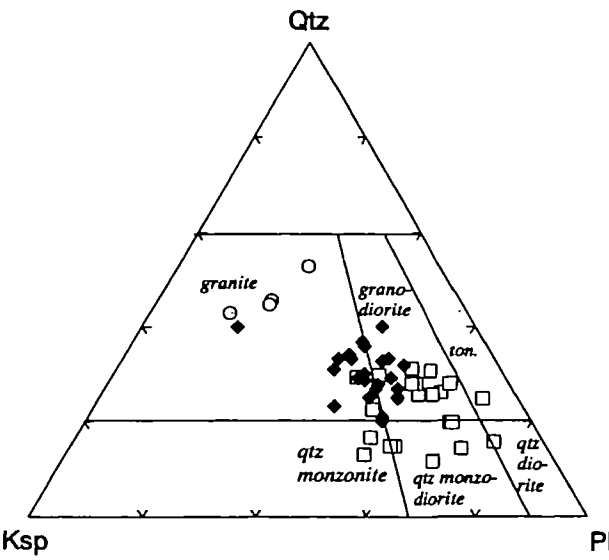

Fig. 3. QAP plot for the rocks of the Cordillera Blanca Bathloith. Open squares, granodiorite, tonalite and various diorites: filled diamonds, leucogranodiorites; open circles, pegmatite–aplite. It should be noted that the diorites, tonalites and granodiorites cannot be distinguished completely on this diagram. Because of this and the similar age (Egeler & De Booy, 1956) they are grouped together.

Amphibole is present in all units, and is associated with clusters of euhedral zircon, apatite, sphene, biotite and magnetite. Compositions vary from magnesiohornblende to ferrohornblende (Petford, 1990) with little change in Al^{iv}, Si and Mg between the different units.

Biotite forms large primary euhedral plates or replaces amphibole. Compositions straddle the phlogopite–annite divide (Petford, 1990) and evolve towards siderophyllite in the acidic rocks. Plagioclase is zoned (An_{58-18}) and is rather sodic, even in the basic rocks (at ~55% SiO_2 An_{49-29}; Petford, 1990). K-feldspar is phenocrystic in the leucogranodiorites, where it can be up to 8·5 cm long and enclose all the other phases.

Muscovite is confined to leucogranodiorite facies rocks, and is of secondary origin. It occurs in the deformed rocks of the western margin within strong, quartz ribbon fabrics (Atherton & Sanderson, 1987; Petford & Atherton, 1992). Mineral compositions are consistent with the textural evidence in that the Ti contents are low, as indicated by Miller *et al.* (1981) for secondary muscovite (Petford & Atherton, 1992).

Two aspects of the mineralogy are important. First, the primary assemblage is metaluminous, containing hornblende, sphene and magnetite. Significantly, muscovite is a late local overprint. Second, although the mineralogy in most respects is similar to that of the Coastal Batholith both modally and compositionally (see Mason, 1985), plagioclase is clearly more sodic and there are no An-rich cores (An>80%) so characteristic of infracrustally derived granites (Chappell & Stephens, 1988). These differences are important and together with the chemistry distinguish the Cordillera Blanca Batholith from the Coastal Batholith.

Syn-plutonic basic dykes and associated mafic enclaves have not been found in the Cordillera Blanca Batholith. One late dyke cutting the roof facies at Llanganuco is ~4 m wide and chilled against the leucogranodiorite. The only other dyke found is a sheared microdiorite, again cutting leucogranodiorite in the Canyon del Pato (Fig. 1, inset). The paucity of evidence for contemporaneous basic magma is a further significant feature in strong contrast to the Coastal Batholith (and most Cordilleran Batholiths), where it is abundant in the form of syn-plutonic dykes, enclaves and mixed rocks (see Pitcher *et al.*, 1985).

AGE OF THE BATHOLITH

K–Ar radiometric ages have been determined by a number of workers (see Cobbing *et al.*, 1981), with values showing a spread of apparent ages between 16·5 and 2·7 Ma. The data apparently define two groups, i.e. 16·5–9 Ma and 6–2·7 Ma. The older ages occur in the southern and eastern margin in tonalites and diorites, and were considered by Stewart *et al.* (1974) to represent intrusion ages. The interpretation of the younger ages (6–2·7 Ma) in the leucogranodiorite is more problematical, not least because the youngest occur along the western deformed margin. Recent $^{40}Ar/^{39}Ar$ dating (Petford & Atherton, 1992) has confirmed a young age (5·18 Ma) at Llanganuco and the older age (9·87 Ma) at the southern end of the batholith (Fig. 1). Uranium–lead zircon data (Mukasa, 1984) from a leucogranodiorite from Llanganuco form an isochron with the relevant intercept at $6·3 \pm 0·3$ Ma, and two fractions from a tonalite from the Carhuish Stock give a 13·7 Ma age (Fig. 1). These more recent data complement the K–Ar data and emphasize the age grouping. $^{40}Ar/^{39}Ar$ data also indicate that ages young from $5·18 \pm 0·5$ Ma at the centre of the batholith to 2·7 Ma towards the western, fault-bounded margin (Petford & Atherton, 1992). This 'younging' is believed to reflect argon loss from deformed and recrystallized micas after granite emplacement. The deformation ages recorded by the muscovite foliation coincide with Quechua 3, the final stage of Pliocene tectonic activity in northern Peru (Mégard, 1989). No ages are available for the granodiorite, which is assigned to the older units following Egeler & De Booy (1956).

The tonalite–quartz diorite facies to the south and on the margins are significantly older than the leucogranodiorite (~8·5 Ma) and therefore they cannot be directly related.

GEOCHEMISTRY

Sixty-six rocks were analysed for major and trace elements by X-ray fluorescence (XRF) and instrumental neutron activation analysis (INAA) (U, Cs, Ta, Hf and Th). Sample collection was determined by accessibility and geological interest, with a concentration along the well-exposed glaciated valleys, perpendicular to the strike of the batholith at Llanganuco, Olleros, Cojup, etc. (Fig. 1). Representative analyses and analytical procedures are given in Table 1.

Major elements

Major element variation diagrams for rocks of the batholith show a large compositional range (52–77% SiO_2). Although there is some scatter, Al_2O_3, TiO_2, MgO, P_2O_5 and CaO all show good negative correlations (Fig. 4). Only K_2O and Na_2O increase with increasing SiO_2, the latter showing a generally flat trend around a mean of ~4 with just a slight increase in the leucogranodiorites (average 4·7%, $n = 32$, range 3·19–5·32).

The granodioritic rocks (67–70% SiO_2) show good trends for MgO, CaO, TiO_2, K_2O and P_2O_5, whereas the tonalitic–dioritic facies with SiO_2 contents <65% show considerable scatter (Fig. 4). Aplites and pegmatites have variable high alkali contents and low MgO, FeO and CaO contents (Fig. 4).

On a K_2O vs SiO_2 plot the rocks define a typical high-K calc-alkaline trend (Fig. 4). Alkali contents are high, with Na_2O ranging from 3·19 to 5·61% and K_2O from 1·86 to 5·83%. On a $K_2O + Na_2O$ vs SiO_2 plot the samples lie on the dividing line between the alkaline and subalkaline field. In contrast, rocks from the Coastal Batholith are subalkalic (see Fig. 8 below). It should be noted that, on a chemical basis, the leucogranodiorites with SiO_2 70–74% (average 71·6%) and $K_2O + Na_2O > 6\%$ classify as granites (Wilson, 1989).

The difference in total alkali chemistry between the two batholiths is due almost entirely to the higher Na_2O content of the Cordillera Blanca suite (see Fig. 8 below), K_2O values being similar to those of the Coastal Batholith. These Na-rich plutonic rocks have only recently been recognized and distinguished from rocks of the more voluminous Coastal Batholith (Atherton & Petford, 1993), although it is clear there are similar rocks throughout the high Andes (e.g. see Parada, 1990). When plotted on an Ab–An–Or normative diagram, they trend from tonalite through granodiorite to a tight group just within the trondhjemite field of O'Connor (1965), although some straddle the boundary and a few lie in the granite field (Fig. 5). The leucogranodiorites are clearly different from granites with a similar SiO_2 range of a typical Cordilleran superunit from the Coastal Batholith (Fig. 5, which evolved by fractionation from tonalite (Atherton, 1984). They are trondhjemites or transitional trondhjemites on the basis of normative classifications. These rocks are singular in that there are also subtle differences in major element chemistry compared with granites (70–74% SiO_2) from typical Cordilleran suites, with lower FeO (total), MgO, TiO_2 and CaO, and significantly higher Al_2O_3 than equivalent rocks from the Coastal Batholith (Figs 6 and 8).

In contrast, the tonalites and granodiorites are similar in some respects to the tonalitic suites of the Coastal Batholith. Thus on an Ab–An–Or classifica-

Table 1: Major and trace element abundances in the batholith rocks

	Leucogranodiorites									
Sample:	880	884	902	900	915	888	925	919	75	76
SiO_2	71·45	72·25	72·14	70·13	72·48	72·27	72·15	71·74	71·8	72·2
TiO_2	0·28	0·2	0·2	0·39	0·2	0·2	0·24	0·22	0·24	0·24
Al_2O_3	14·64	14·69	14·59	15·01	14·54	14·7	15·15	14·95	15·27	15·05
Fe(T)	1·09	0·84	3·34	1·77	0·75	0·99	0·79	1	1·03	1·01
MnO	0·04	0·04	0·07	0·05	0·05	0·05	0·04	0·06	0·05	0·06
MgO	0·16	0·17	1·66	0·86	0·11	0·08	0·22	0·2	0·21	1·68
CaO	1·92	3·12	1·76	2·75	1·7	1·56	1·82	1·84	1·94	1·9
Na_2O	4·74	4·85	3·19	4·26	5·02	4·8	4·66	4·88	4·86	3·67
K_2O	3·61	3·68	3·2	3·48	3·55	3·88	3·88	3·66	3·48	3·26
P_2O_5	0·08	0·05	0·05	0·08	0·05	0·05	0·1	0·05	0·07	0·09
LOI	0·52	0·46	0·6	0·8	0·61	0·52	0·76	0·66	0·4	0·41
Total	98·53	100·3	100·8	99·58	99·06	99·1	99·81	99·26	99·35	99·57
Or	21·3	21·7	18·9	20·6	21	22·9	22·9	21·6	20·1	19·3
Ab	40·1	41	27	36	42·3	40·6	39·4	41·3	41·1	31
An	8	7·4	8·4	11·6	6·6	7·1	8·4	8·1	9·2	8·8
Ba	673	816	664	619	592	739	778	864	780	728
Ce	47	†	33	†	38	46	50	26	41	38
Co	75	58	58	81	74	67	84	68	67	77
Cr	9	41	38	98	97	39	34	133	10	9
Cs*	5·8	1·31	3·17	6·29	2·1	2·2	5	3·61	3·1	2·05
Eu*	0·84	†	1·21	†	0·7	0·7	1	—	—	—
Hf*	3·6	2·72	2·13	3·14	2·8	4·1	3·2	3·35	4·56	3·22
La	16	†	20	†	12	18	18	14	26	22
Nd	20	†	21	†	17	19	18	17	26	24
Ni	18	18	31	18	30	16	15	50	7	8
Pb	19	18	17	17	22	20	23	19	21	20
Rb	143	133	81	122	119	122	141	133	100	135
Sc	2	2	4	1	2	2	2	2	4	4
Sm*	3·58	†	3·36	†	2·7	3·1	3·3	4·8	6·2	4·96
Sr	456	427	440	463	380	355	471	491	566	530
Ta*	2·16	1·39	0·79	1·48	1·7	1·4	1·8	2·3	2·18	1·96
Tb*	0·31	†	0·18	†	0·29	0·35	0·32	0·33	0·47	0·44
Th*	9·9	10·9	20·4	16	10	12	11	7	12·5	11·5
U*	3·01	1·76	6·37	9·87	2·7	1·4	3·3	4·27	4·83	2·85
V	18	11	75	30	—	—	—	12	15	16
Y	8	8	7	6	7	12	7	12	9	8
Zn	53	29	60	59	—	—	—	50	34	43
Zr	131	103	99	103	82	94	105	116	142	112

Table 1: continued

	Leucogranodiorites						Pegmatites			
Sample:	84	924	927	64	93	69	885	916	77	92
SiO_2	70·66	71·13	71·72	72·25	72·15	71·21	74·96	77·04	75·59	74·7
TiO_2	0·23	0·23	0·28	0·28	0·19	0·25	0·1	0·11	0·13	0·1
Al_2O_3	15·79	14·86	14·68	14·98	15·22	14·53	13·91	13·08	13·87	14·68
Fe(T)	1·17	1·04	1·1	1·09	0·85	1·9	0·24	0·45	0·55	0·71
MnO	0·06	0·06	0·04	0·06	0·09	0·05	0·13	0·04	0·04	0·16
MgO	0·24	0·19	0·24	0·5	0·14	0·1	<0·1	<0·1	<0·1	<0·1
CaO	2·08	1·87	2·04	1·96	1·72	1·83	0·58	1·11	0·93	0·61
Na_2O	5·32	4·95	5·02	4·85	5·19	5·13	4·43	5·36	5·01	5·07
K_2O	3·38	3·42	3·18	3·29	3·23	3·12	4·32	2·52	4·04	3·84
P_2O_5	0·07	0·06	0·07	0·08	0·05	0·06	0·08	0·04	0·04	0·04
LOI	0·69	1·91	1·37	0·19	0·62	1·09	0·71	0·07	0·04	0·12
Total	99·69	99·72	99·74	99·53	99·45	99·27	100·5	99·83	100·3	100
Or	20	20·2	18·9	19·4	19·1	18·4	25·3	14·9	23·8	22·7
Ab	45	4·19	42·3	41	41·6	43·4	37·5	45·3	42·4	42·9
An	9·2	8·2	8·1	9·1	11·8	6·9	2·3	4·2	3·4	2·8
Ba	813	697	473	672	693	357	29	42	121	<0·1
Ce	42	27	38	37	27	†	8·4	2	7	50
Co	59	64	68	57	68	74	64	78	57	40
Cr	9	37	34	12	8	6	103	114	8	5
Cs*	1·35	—	—	—	—	—	1·2	2·9	—	—
Eu*	—	—	—	—	—	†	<0·1	1	—	—
Hf*	3·76	—	—	—	—	—	1·27	0·2	—	—
La	27	17	19	23	17	†	4	1	4	5
Nd	24	16	23	21	17	†	7	6	7	36
Ni	4	16	16	4	4	5	41	43	6	2
Pb	17	21	22	17	20	21	15	18	21	25
Rb	101	135	149	100	155	161	207	104	145	43
Sc	4	1	3	4	3	1	2	2	2	5
Sm*	4·45	—	—	—	—	†	0·71	0·1	—	—
Sr	570	461	419	532	389	368	41	102	60	<0·1
Ta*	1·41	—	—	—	—	—	3·57	3·4	—	—
Tb*	0·32	—	—	—	—	†	0·18	0·12	—	—
Th*	10·2	9	16	9·4	8·4	11·5	5	0·84	8·3	7·2
U*	2·52	—	—	—	—	—	9·6	5·2	—	—
V	16	13	18	26	9	17	3	5	4	5
Y	9	15	11	5	10	9	8	5	22	35
Zn	30	58	58	57	68	55	10	13	6	13
Zr	137	119	118	125	81	104	22	1	23	572

(continued on next page)

Table 1: continued

	Quartz diorites				Tonalites					Dyke
Sample:	63	901	905	906	903	68	910	914	928	86
SiO_2	51·61	55·03	58·54	56·47	61·71	63·37	63·41	68·38	69·37	54·36
TiO_2	0·99	1·27	0·92	1·21	0·98	0·79	0·71	0·44	0·45	1·08
Al_2O_3	18·12	16·94	17·87	16·11	15·83	16·22	16·85	15·63	15·4	17·16
Fe(T)	7·35	7	5·04	7·3	5·35	3·81	3·56	3·16	2·23	8·44
MnO	0·12	0·1	0·07	0·1	0·08	0·09	0·08	0·06	0·06	0·1
MgO	4·72	4·02	2·7	4	3·46	2·06	1·82	1·28	0·8	3·5
CaO	7·39	6·98	5·76	6·47	5·24	4·54	4·27	3·17	3·2	5·89
Na_2O	3·94	3·61	4·24	3·61	3·82	4·12	4·1	4·11	3·82	4
K_2O	1·68	2·24	2·02	1·99	1·98	2·32	2·44	2·98	3·59	2
P_2O_5	0·22	0·38	0·3	0·37	0·23	0·19	0·19	0·12	0·15	0·26
LOI	3·46	2·12	2·04	3·01	2·04	1·59	1·99	0·9	1	4·01
Total	99·6	99·69	99·5	100·6	100·7	99·1	99·42	100·2	100·0	100·8
Or	9·9	13·2	11·9	11·8	11·7	13·7	14·4	17·6	21·1	11·8
Ab	33·3	30·4	35·9	30·5	32·3	34·9	34·7	34·8	32·3	33·8
An	26·8	23·4	23·8	21·9	20·2	18·9	19·9	14·9	14·2	23
Ba	412	722	664	567	410	474	602	748	704	477
Ce	33	†	†	44	†	†	27	38	20	38
Co	40	46	52	51	56	48	51	53	52	37
Cr	86	59	39	55	62	9	63	39	28	88
Cs*	5·1	3·8	3·7	3·3	2·98	—	2·12	1·4	5·3	2
Eu*	1·25	†	†	1·6	†	†	1·05	1·3	0·8	1·23
Hf*	3·26	2·61	4·4	3·5	3·56	—	4·06	3·8	3·3	4·35
La	17	†	†	28	†	†	22	18	15	22
Nd	26	†	†	35	†	†	16	16	17	33
Ni	19	20	20	21	20	19	19	18	20	21
Pb	9	11	12	4	3	10	9	7	22	3
Rb	68	71	65	64	62	94	91	119	133	46
Sc	24	15	7	16	12	7	6	5	2	18
Sm*	4·93	†	†	6·3	†	†	3·9	4	2·5	4·78
Sr	743	895	969	943	711	627	755	573	583	398
Ta*	0·75	0·83	1·3	0·79	2·5	—	0·76	1·7	1·3	1·37
Tb*	0·51	†	†	0·55	†	†	0·27	0·47	0·27	0·75
Th*	2	8·7	13	3	5·43	6	18·5	11	25	4
U*	1·02	3·8	3·1	2·6	2·5	—	2·43	3·3	3	1·75
V	200	181	121	173	138	99	92	47	34	153
Y	16	14	11	15	12	10	7	13	8	26
Zn	117	112	89	125	96	93	118	82	76	118
Zr	114	141	144	142	118	115	140	107	123	161

Major and trace element analyses by XRF.
*Data by INAA. †See Table 2.

The analysed rocks are fresh with little alteration apart from the cataclasites near the western contact. Minor chloritization of hornblende and biotite is not uncommon but in 85% of cases it makes up <1% by volume and is often much less. K-feldspar and plagioclase are rarely altered. In the rocks of the western margin the deformation is strongly partitioned into quartz zones, the feldspars showing brittle fracture but little or no alteration. Sericitization of plagioclase is uncommon. One rock not included in the graphs is a strongly sheared rock with an anomalous chemistry in both major and trace elements, e.g. very low CaO, V and Sr and very high Rb, compared with equivalent rocks. It has values well away from the general trends. The lack of a similar pattern of values and the consistent pattern in Rb, V and La, for example, suggest that the scatter in some elements is not due to late-stage alteration.

Major elements were determined by analysis of glass fusion discs using the method of Norrish & Hutton (1969), and trace elements on pressed powder pellets with the corrections of Brown *et al.* (1973). Relative deviation of the major elements was <1·5% for SiO_2, TiO_2, Al_2O_3, Fe_2O_3, CaO, Na_2O and K_2O, 2·5% for MnO, 3% for MgO and 15% for P_2O_5. Deviations from G_2 [Standard value − analysed value (4)] are SiO_2 0·15; TiO_2 0·0; Al_2O_3 0·0; Fe_2O_3 0·11; MnO 0·07; MgO 0·02; CaO 0·11; Na_2O 0·07; K_2O 0·01; P_2O_5 0·01.

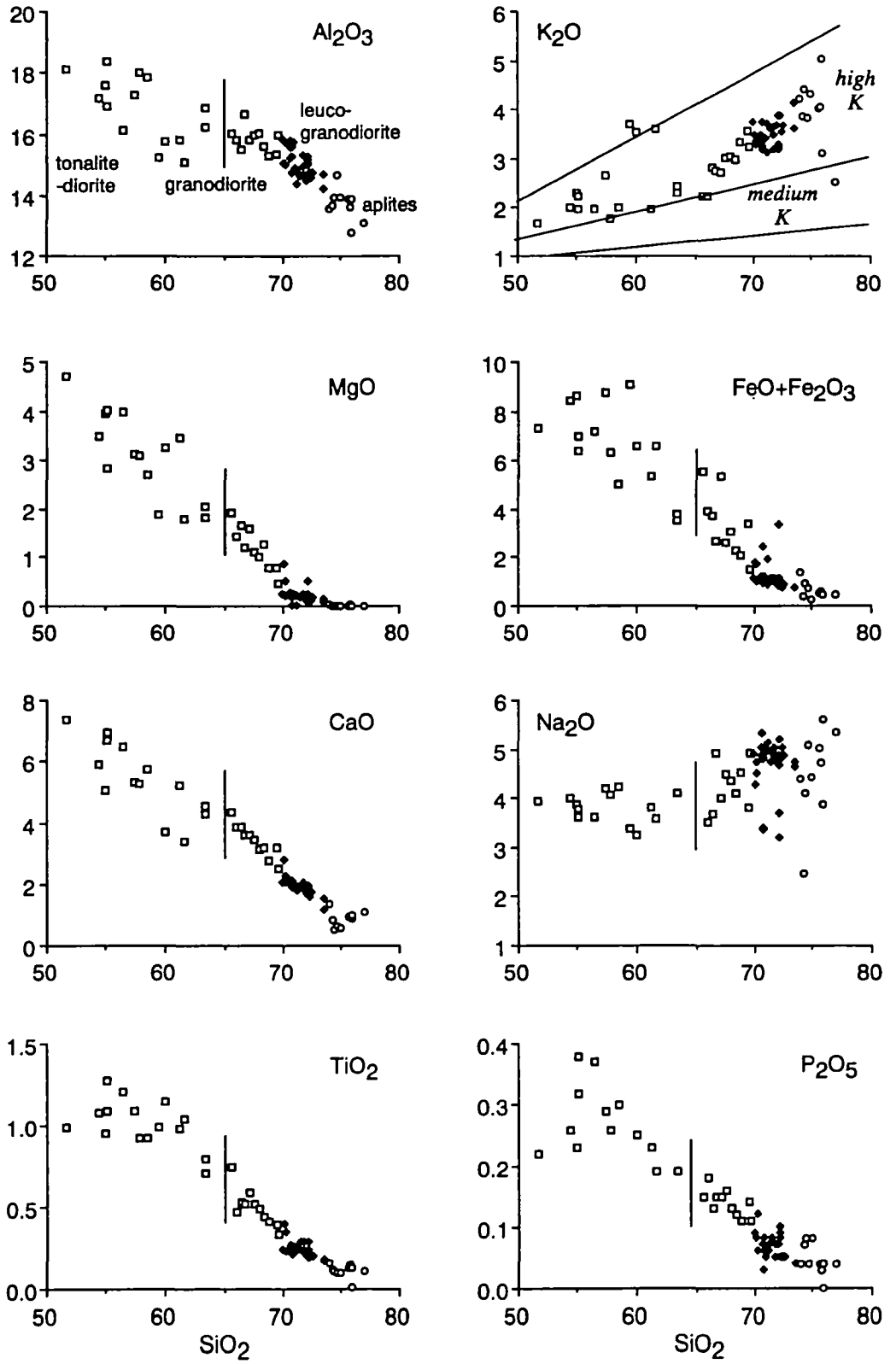

Fig. 4. Harker diagrams for major elements in rocks from the Cordillera Blanca Batholith; symbols as in Fig. 3. Guide lines are drawn to separate granodioritic rocks showing coherent trends in MgO, CaO, TiO_2, P_2O_5 (65–70% SiO_2) from the tonalites and diorites which are of similar age. The K_2O vs SiO_2 plot indicates the high-K character of the batholith.

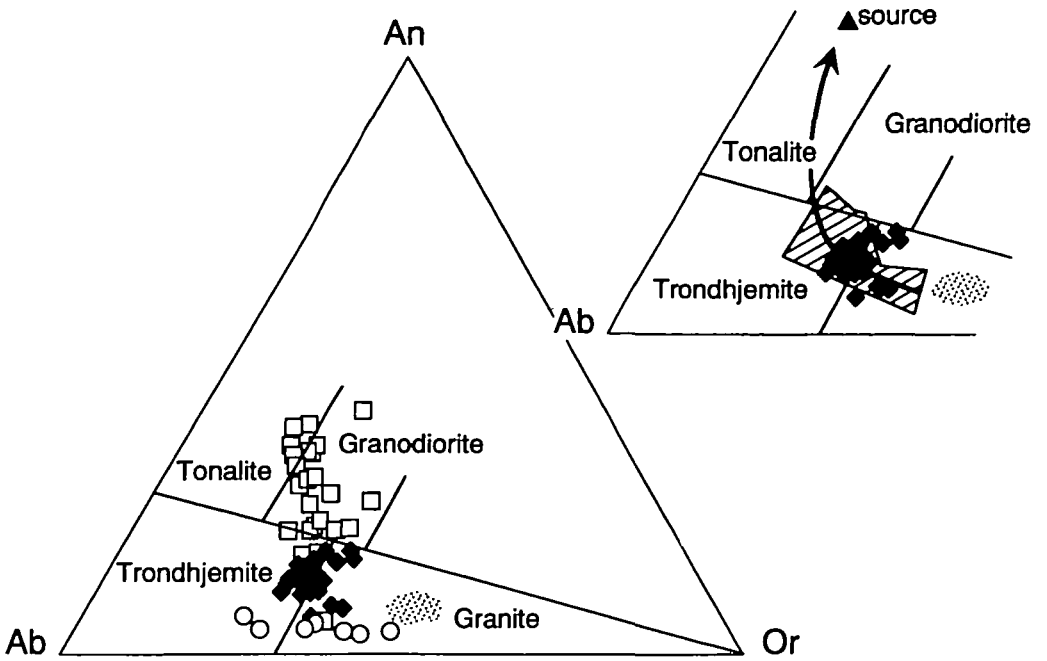

Fig. 5. An–Ab–Or diagram showing the trondhjemitic character of the leucogranodiorites and the tonalitic, granodioritic character of the more basic rocks. Fields from O'Connor (1965). Fractionated granites (>70% SiO_2) from the Santa Rosa Super Unit of the Coastal Batholith have compositions in the stippled field. Symbols as in Fig. 3. Inset shows Cordillera Blanca leucogranodiorites, Coastal Batholith granite field and the field (diagonal lines) for experimental melt compositions (Sen & Dunn, 1994) from amphibolite dehydration at 1·5 and 2·0 GPa, with the arrow showing the change in composition of melts with increasing temperature. Filled triangle is the experimental starting composition (= source). The amphibolite assemblage was amphibole, plagioclase, quartz, ilmenite and garnet.

tion diagram they also lie in the tonalite–granodiorite field (Fig. 5). None the less, compared with those of the Coastal Batholith they have slightly lower CaO and MgO, and higher $Na_2O + K_2O$ (Fig. 8) contents comparable with the leucogranodiorites, but the Al_2O_3 contents (see Fig. 8) are the same or lower and the TiO_2 contents higher.

Trace elements

Trace elements show good correlations with SiO_2 for some elements such as V but diffuse trends for Sr, Ba and Rb (Fig. 7). Generally the trace elements show far more scatter than the major elements, and even the granodioritic rocks show little coherent variation (Fig. 7). Rb/Sr increases very slightly (from 0·18 to 0·59) over the range 52–73% SiO_2, whereas K/Rb shows significant scatter about a mean of ~250 over the same SiO_2 range. Importantly, Sr is enriched and Y is depleted in the Cordillera Blanca rocks relative to similar rocks in the Cordillera Batholith [Fig. 8 and Atherton & Sanderson (1985)].

Aplites and pegmatites with SiO_2>74% [DI (normative quartz + orthoclase + albite) >90], are characterized by marked depletions in Sr, Ba, La, Ce, Nd, Zr, Hf and Zn relative to the more basic facies (Fig. 7, Table 1).

Rare earth elements

Eighteen rocks spanning the range of SiO_2 (55–73·6%) of the batholith were analysed for REEs (by radiochemical neutron activation analysis, Table 2). La_N/Yb_N ratios range from 3·3 to 77. The leucogranodiorites are strongly depleted in heavy REE (HREE) compared with the more basic rocks (quartz diorite–tonalite), but there is overlap in the light REE (LREE) from La to Pr although the leucogranite field lies at lower values (Fig. 9). Leucogranodiorite 884 from Paron (Fig. 1) has the lowest REE abundances and highest La_N/Yb_N ratio (77) of all the rocks. The variation within the leucogranodiorite facies is large (Fig. 9). La_N/Yb_N varies from 19 to 77 over an SiO_2 range of 3%, in rocks which crop out over a distance of 140 km. Only one sample (69) exhibits a negative Eu anomaly. A plot of La_N/Yb_N vs SiO_2 shows a steady increase in La_N/Yb_N ratio in the basic–intermediate facies, i.e. with SiO_2 contents up to ~65%, then considerable scatter in the leucogranodiorites and granodiorites (Fig. 10). The consistent variation in rocks below 65% is due to a decrease in the HREE (e.g. Lu_N varies from 10 to near 2·2; Fig. 9) with increasing silica content; a feature implying a consistent change in source mineralogy or amount of melt with time,

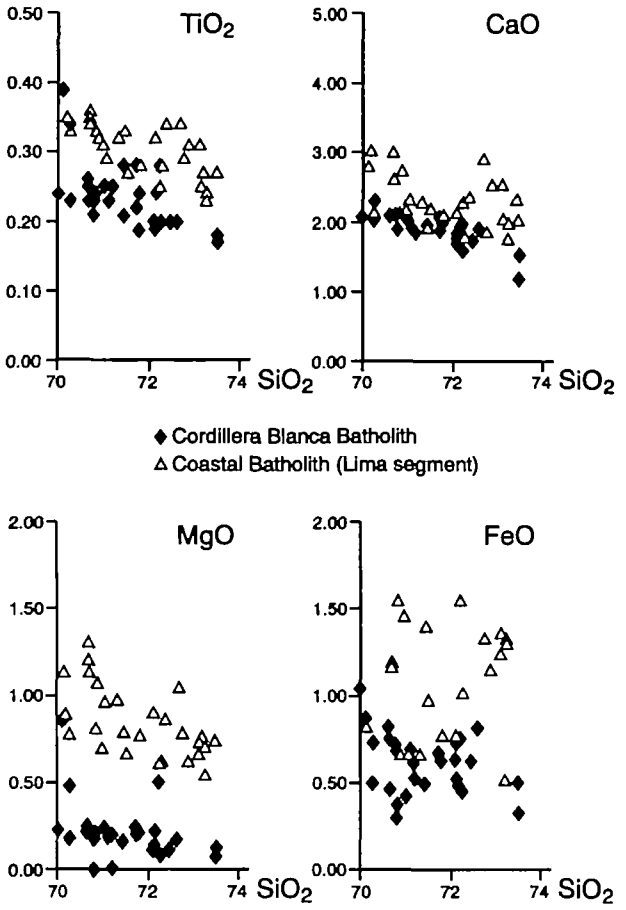

Fig. 6. Harker plots of MgO, TiO_2, CaO and FeO of the leucogranodiorites of the Cordillera Blanca Batholith and granites of the Coastal Batholith [data from Atherton (1984, and unpublished)].

or fractionation of a phase such as garnet with a high K_D for the HREE.

Radiogenic isotopes and the source of the magmas

Sr (whole rock) and Pb isotopic data for separated feldspars from the Cordillera Blanca Batholith have been discussed by Atherton & Sanderson (1987) based on the work of Mukasa & Tilton (1984) and Beckinsale *et al.* (1985), who thought the ultimate source could well be enriched subcontinental lithosphere. The Cordillera Blanca rocks (tonalite, granodiorite, leucogranodiorite) define a compact group with very similar Pb isotope compositions to the gabbros, diorites and tonalites of the Lima segment of the Coastal Batholith (Fig. 11), which lies in thin crust to the west, and to the NVZ (Northern Volcanic Zone) lavas of the Andes. They do not appear to contain an old Precambrian crustal component such as the Arequipa massif (Fig. 11, see also oxygen isotopes). Thus the trend towards low $^{206}Pb/^{204}Pb$ observed in CVZ (Central Volcanic Zone) rocks between 16° and 18°S, commonly interpreted as a mixing between mantle-derived Pb and less radiogenic crustal Pb (Davidson *et al.*, 1991) is not seen in the Cordillera Blanca rocks. This may not be surprising, as the Precambrian Arequipa massif is now not thought to make up lower crust north of Lima (Atherton, 1990). Nor do they appear to lie on a mixing line between Nazca plate mid-ocean ridge basalt (MORB) and Pacific sediments. They are enriched in ^{207}Pb relative to MORB and very similar to the homogeneous reservoir of Tilton & Barreiro (1980) which was the source of plutonic and volcanic rocks in central Chile, and which they thought was enriched subcontinental lithospheric mantle.

More recent Sr–Nd work on selected batholith rocks shows relatively small variations in $^{87}Sr/^{86}Sr$ (0·7047–0·7057) and $^{143}Nd/^{144}Nd$ (0·5126–0·5125) ratios (Petford *et al.*, 1996). The older (16–10 Ma) quartz diorites and tonalites define a tight group with ε_{Nd} varying from +0·2 to a most enriched value of −0·2 over a silica range of 14 wt % (Fig. 12). The younger (6–5 Ma) leucogranodiorites are less tightly grouped and slightly more evolved (mean ε_{Nd} $-1{\cdot}38 \pm 0{\cdot}6$, max ε_{Nd} −2·5) than the quartz diorites–tonalites (Fig. 12). However, they are more primitive than the baseline CVZ volcanic andesites (Fig. 12), which Davidson *et al.* (1991) considered could be partial melts of subcontinental lithospheric mantle.

To sum up, the lead data are consistent with a source similar to that of the NVZ, i.e. a subduction modified mantle with very minor crustal contamination (Wilson, 1989), whereas the slightly enriched Sr and Nd data compared with the NVZ lavas suggest involvement of a young crustal component in the petrogenesis of the magmas, especially the leucogranodiorites, which may have been locally derived from the envelope rocks. However, the major component is considered to be mantle derived (see Mukasa & Tilton, 1984).

CAUSES OF CHEMICAL VARIATION IN THE BATHOLITH

Although it is clear that the difference in age and initial Sr and Nd isotope compositions (Fig. 12) preclude the direct derivation of the leucogranodiorites from the tonalites–quartz diorites the major element trends in Harker diagrams show a regularity similar to that seen in fractionating systems (particularly for the granodiorites, Fig. 4). It

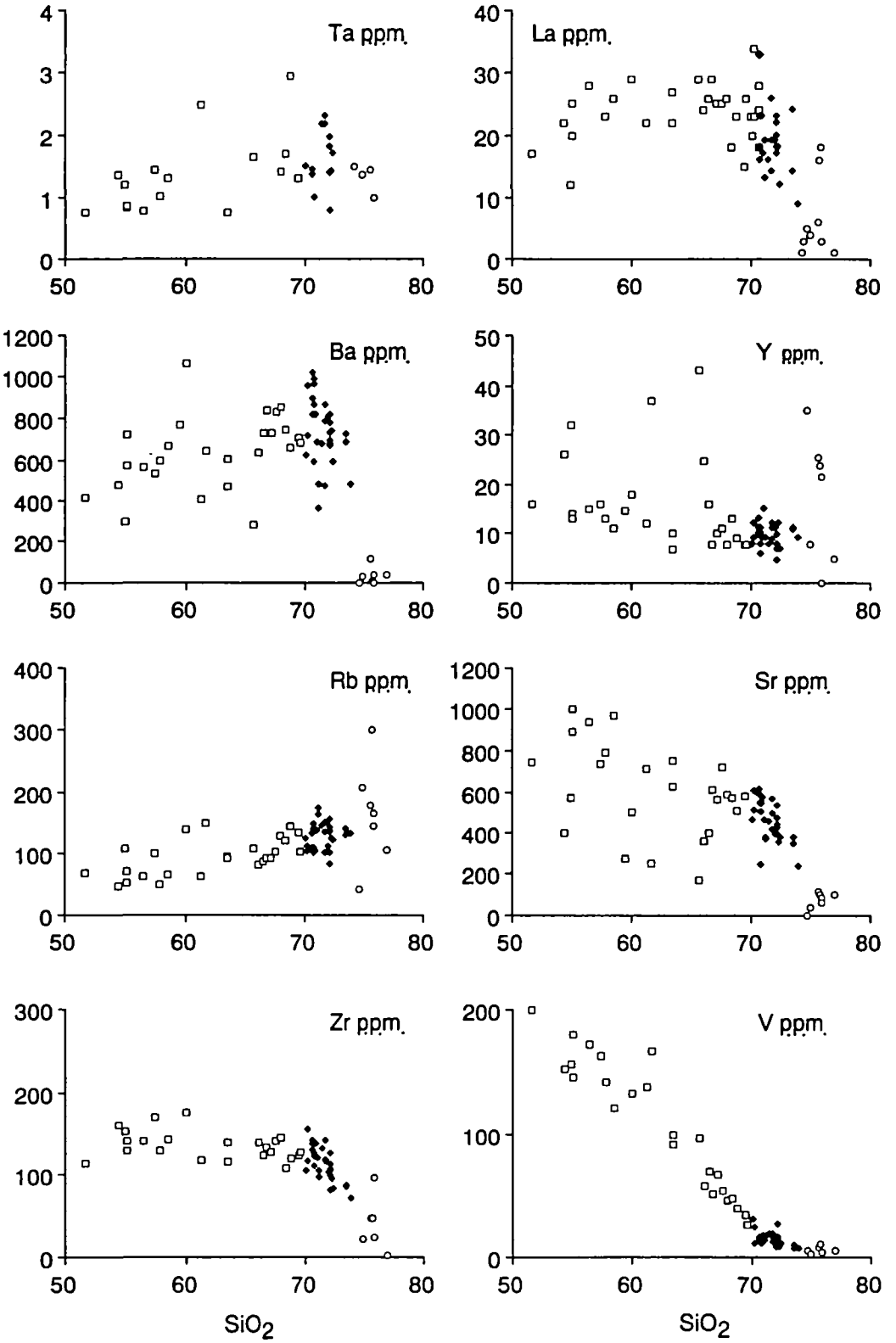

Fig. 7. Harker diagrams for selected trace element contents of rocks of the Cordillera Blanca Batholith; symbols as in Fig. 3. [Note the lack of consistent variations (apart from V) in the granodiorite and even more so in the leucogranodiorite.]

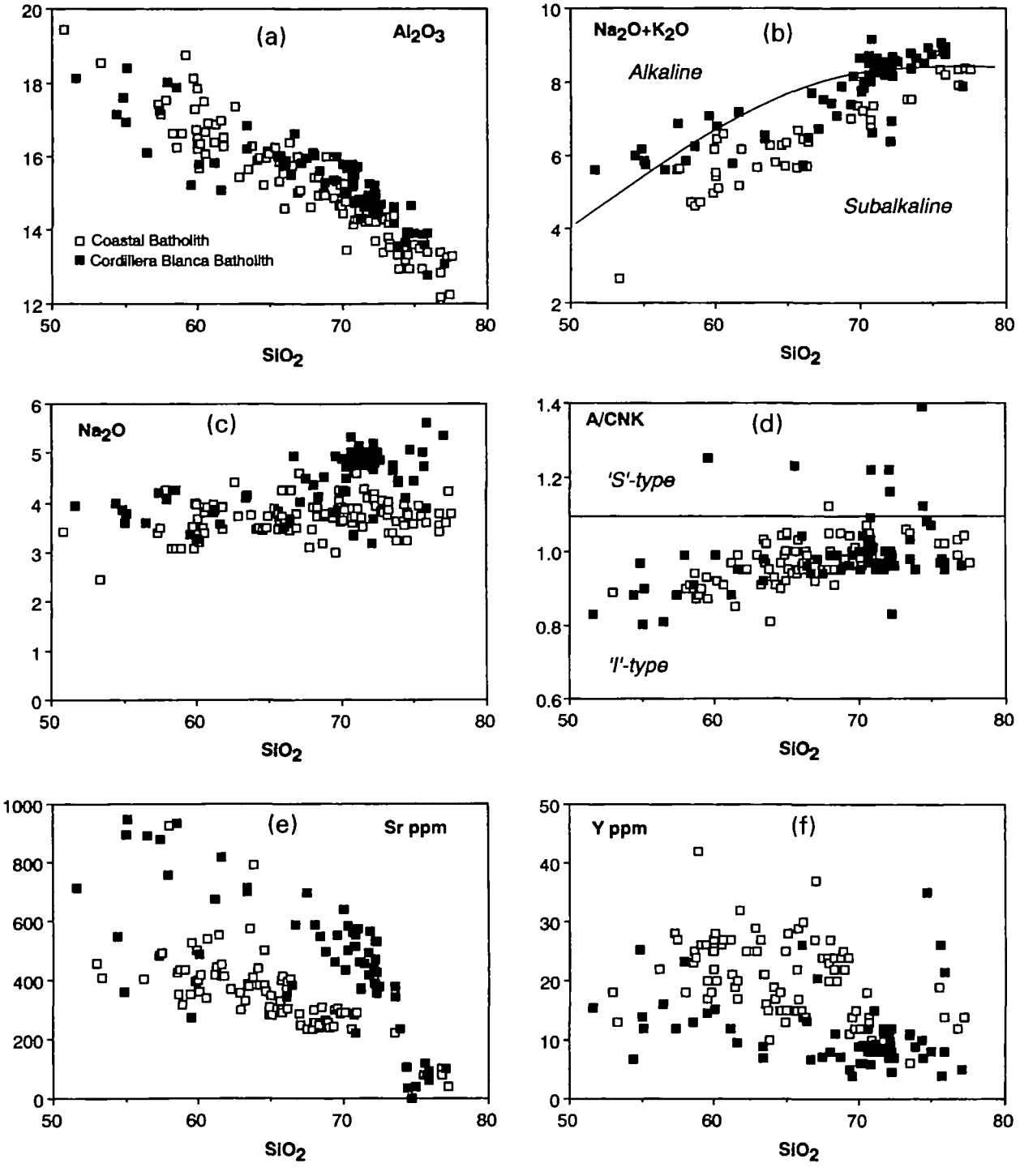

Fig. 8. Plots of (a) Al_2O_3, (b) $Na_2O + K_2O$, (c) Na_2O, (d) A/CNK, (e) Sr and (f) Y, vs SiO_2 for rocks of the Cordillera Blanca and Coastal Batholiths. (Note the slightly alkalic nature of the Cordillera Blanca Batholith, its mainly metaluminous nature and the distinctive chemical character of the batholith in terms of Al_2O_3, Na_2O, Sr and Y compared with the Coastal Batholith.)

might be argued therefore that the acid magmas fractionated from consanguineous mafic magmas at depth (by an AFC process to account for the difference in $^{87}Sr/^{86}Sr$). However, field evidence of subsolidus deformed tonalite and granodiorite enclaves within undeformed leucogranodiorites does not support the proposition that the leucogranodiorite fractionated from more basic rocks at

Table 2: REE abundances (p.p.m.) in selected batholith rocks

	La	Ce	Pr	Nd	Sm	Eu	Gd	Tb	Dy	Yb	Lu
900 (L)	21·4	43·7	4·1	15·7	2·3	0·61	1·55	0·19	1·2	0·3	0·06
884 (L)	19·8	42·2	4·4	15·3	2·7	0·55	1·39	0·17	0·8	0·17	0·03
69 (L)	16·7	37·8	4·3	14·3	2·9	0·47	1·7	0·27	1·5	0·62	0·08
901 (QD)	23·9	51·1	5·9	26·6	5·9	1·53	3·72	0·49	3	0·73	0·13
905 (QD)	24·1	60·4	7·4	26·3	4·7	1·29	3·1	0·38	2·3	0·69	0·12
68 (T)	22·3	54·6	6·4	25·2	4·5	1·2	3	0·40	1·9	0·5	0·08
96 (T)	26	57·4	5·5	21·2	3·3	0·76	2·1	0·22	1·2	0·43	0·07
903 (T)	20·9	45·5	5	19·7	5	1·05	2·54	0·34	1·9	0·6	0·08

L, leucogranodiorite; QD, quartz diorite; T, tonalite. REE determination involved irradiation, radiochemical group separation of REE and γ spectrometry using a Ge (Li) detector, all at Northern Universities Reactor Centre, Risley. Procedure and spectral analysis have been given by Duffield & Gilmore (1979). AGVI was used as a primary standard and results of the analysis of this standard reference are (literature values in parentheses): La 35 (35), Ce 62 (63), Pr 8 (7), Nd 33 (39), Sm 5·2(5·9), Eu 1·5 (1·7), Gd 4·0 (5·5), Tb 0·6 (0·7), Dy 3·5 (3·5), Ho 0·5 (0·6), Er 1·3 (1·2), Yb 1·5 (1·7), Lu 0·2 (0·3).

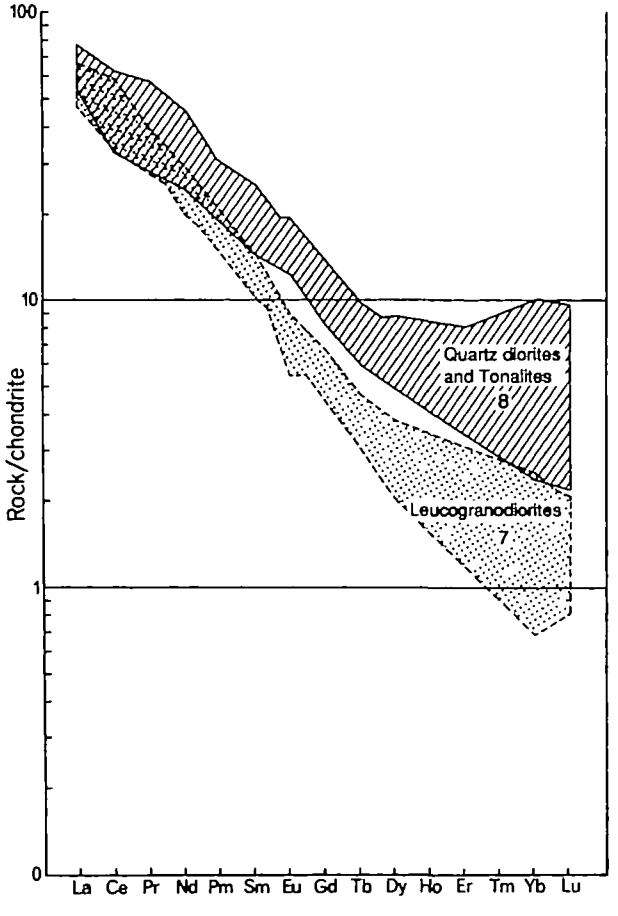

Fig. 9. Chondrite-normalized REE plots for rocks of the Cordillera Blanca Batholith. Envelopes shown for quartz diorites and tonalites ($n = 8$) and leucogranodiorites ($n = 7$).

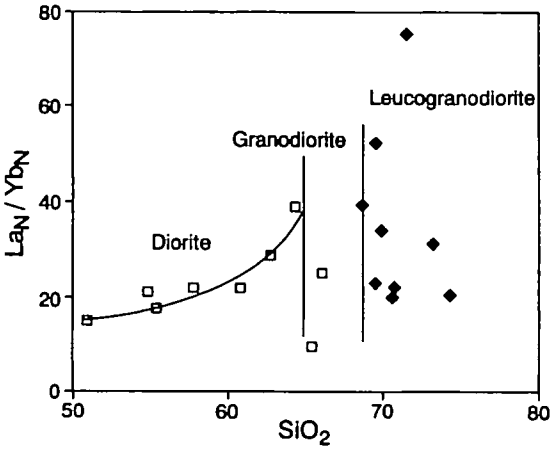

Fig. 10. Plot of La_N/Yb_N vs SiO_2 for rocks of the Cordillera Blanca Batholith. Symbols as in Fig. 3. Guide lines separate the granodiorites (65–70% SiO_2). (Contrast the coherent increase in La_N/Yb_N in the rocks with SiO_2 <65% with the incoherent variation in the granodiorites and leucogranodiorites.)

depth represented by these samples (Atherton & Sanderson, 1987). Furthermore, on a multielement diagram (Fig. 13) there are none of the large ion lithophile element (LILE) enhancements or depletions seen in similar rocks (~72% SiO_2) from the Coastal Batholith which contain the same major mineral phases in similar proportions and which are considered to have evolved by crystal fractionation from a mafic precursor (Atherton & Plant, 1985; Atherton & Sanderson, 1985).

Other evidence, such as the low Rb/Sr in the leucogranodiorites (maximum 0·5, average, 0·29)

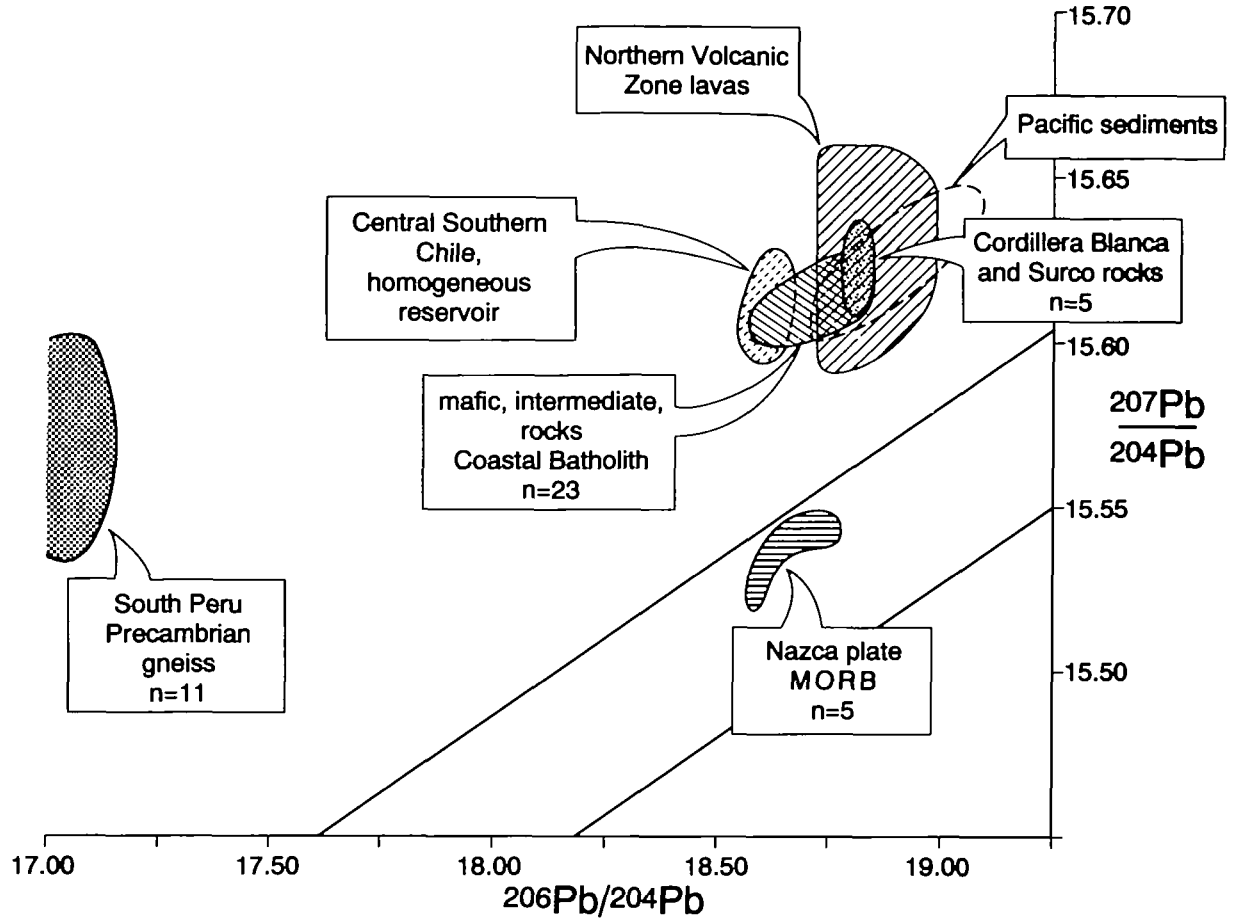

Fig. 11. $^{207}Pb/^{204}Pb$ vs $^{206}Pb/^{204}Pb$ correlation diagram for separated feldspars, [data from Mukasa (1984)], from the Cordillera Blanca Batholith. Also included are fields for southern Peru Precambrian gneiss, the Lima segment rocks of the Coastal Batholith, Nazca plate MORB, the central Chile homogeneous reservoir of Tilton & Barreiro (1980), and Northern Volcanic zone (NZV) lavas [data from Wilson (1989) and Davidson *et al.* (1991)]. Significant differences between the highest and lowest values of $^{206}Pb/^{204}Pb$, $^{207}Pb/^{204}Pb$, $^{208}Pb/^{204}Pb$ for the Cordillera Blanca feldspars are only 0·13%, 0·24% and 0·61%. Included in the Cordillera Blanca field are two rocks from the related Surco stock (21 Ma) to the south, which have SiO_2 contents near 60%, contain hornblende and sphene, and have an A/CNK value near 0·86. They do not appear to have a different source, and are similar to the Carhuish tonalite included here. The coherence of these data on the Pb isotope plot indicates that even the deformed rocks have not been significantly disturbed.

compared with >2·0 in equivalent Coastal Batholith rocks which vary consistently with SiO_2 content (Atherton, Fig. 7, 1993), and the lack of an Eu anomaly are not consistent with an origin by crystal fractionation. The volume of leucogranodiorite (>85% by volume of the batholith: minimum 6000 km^3) is in marked contrast to that of rocks with similar SiO_2 contents in the Coastal Batholith (~10% by volume, Atherton, 1984), and generation by fractionation from basalt would produce an amphibole–clinopyroxene–garnet residue (see Fig. 19 below), for which there is no evidence, of 54 000 km^3 at the site of crystallization (Spulber & Rutherford, 1983). Thus there appears to be no simple scheme involving fractionation of a dioritic or more mafic magma source to form the leucogranodiorites of the batholith. Even within the main leucogranodiorite facies there is little evidence of compositional continuity which would indicate an important role for crystal fractionation. Thus there is a large spread and no consistent variation in rock trace element contents, e.g. REE, Ba and Y, over the SiO_2 range 70–74% (Fig. 7). Furthermore, whole-rock Rb–Sr isotopic data fail to define isochrons, which indicated to McCourt (1978) and Mukasa (1984) that the leucogranodiorite was made up of batch melts from a heterogeneous source.

Oxygen isotopes, deformation and magma sources

Oxygen isotopes have proved useful in distinguishing

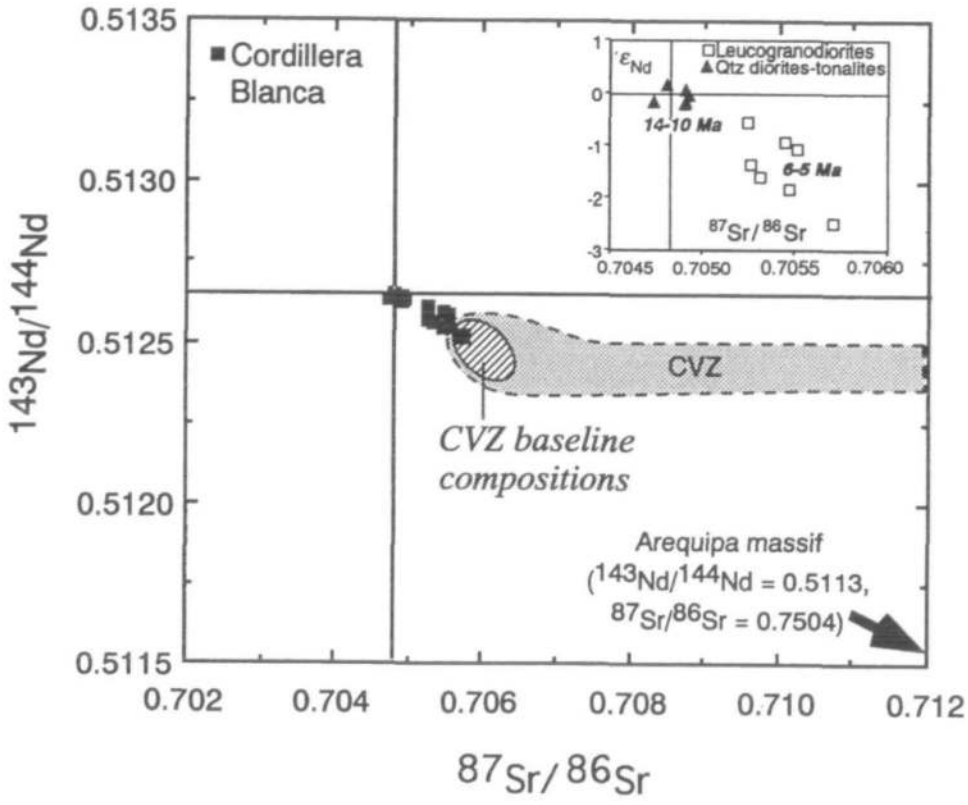

Fig. 12. Plot of $^{143}Nd/^{144}Nd$ vs $^{87}Sr/^{86}Sr$ for Cordillera Blanca Batholith rocks. The field of Miocene to Recent lavas from the Central Volcanic Zone (CVZ) is also shown, as well as that for the Precambrian Arequipa massif. Data from Davidson *et al.* (1991) and Mukasa (1984), respectively. The CVZ baseline compositions, i.e. the last isotopically evolved basaltic andesites from this zone, are more evolved than all but one of the Cordillera Blanca rocks. There is none of the extreme enrichment in isotopic composition characteristic of the CVZ magmas. Inset shows the isotopic composition of the batholith rocks with respect to age. The older (14–10 Ma) quartz diorites and tonalites have compositions which cluster around bulk Earth. The shift towards more negative ε_{Nd} and higher $^{87}Sr/^{86}Sr$ ratios in the younger (6–5 Ma) leucogranodiorites is consistent with derivation from an enriched source in subcontinental lithosphere with a minor upper-crustal component.

magma source regions and assessing the extent of crustal involvement and late-stage fluid–rock interaction in granite petrogenesis (Taylor, 1986). In general, melts formed directly from the mantle, or indirectly by partial melting of unweathered metabasaltic material, will have $\delta^{18}O$ values of 5–6‰. In granitic rocks derived by partial melting of metasedimentary protoliths $\delta^{18}O$ is generally $>+10$‰ [Taylor (1986) and Fig. 14].

The oxygen isotope compositions of 15 quartz and mica (biotite and muscovite) mineral separates and their host rocks from an ~5 km east–west traverse along the Llanganuco section of the batholith into the Cordillera Blanca fault zone (Fig. 1), together with a further 17 whole rocks (granitic rocks, Chicama sediments and metasedimentary xenoliths) from the Cordillera Blanca are given in Table 3.

The leucogranodiorite cataclasite 921 is from the fault-bounded western margin of the batholith (Fig. 14). Analyses were made both of quartz grains within the cataclasite matrix, and the deformed matrix itself. X-ray diffraction (XRD) analysis shows that the matrix (mean grain size <100 μm) is made up of quartz and albite, with minor chlorite and illite. The deformed leucogranodiorite (918) from inside the fault zone contains secondary muscovite related to deformation and was partially mylonitized during and after magma emplacement (Petford & Atherton, 1992). The undeformed leucogranodiorite (879) is from the interior of the batholith. A sample of undeformed Yungay ignimbrite (889) and a garnet-bearing pegmatite (92) from outside the fault margin were analysed for comparison with the batholith rocks.

The range in isotopic composition of the batholith minerals is bracketed by biotite and quartz. In general, there is a decrease in $\delta^{18}O$ quartz from about +11 to +9·2‰ towards the Cordillera Blanca fault (Fig. 14). Similar trends, although not as pronounced, are seen in biotite (+6·1 to +5·7‰ and whole rock (+9·2 to +8·7‰). The cataclasite matrix has a slightly lower $\delta^{18}O$ value (+8·2‰) than both

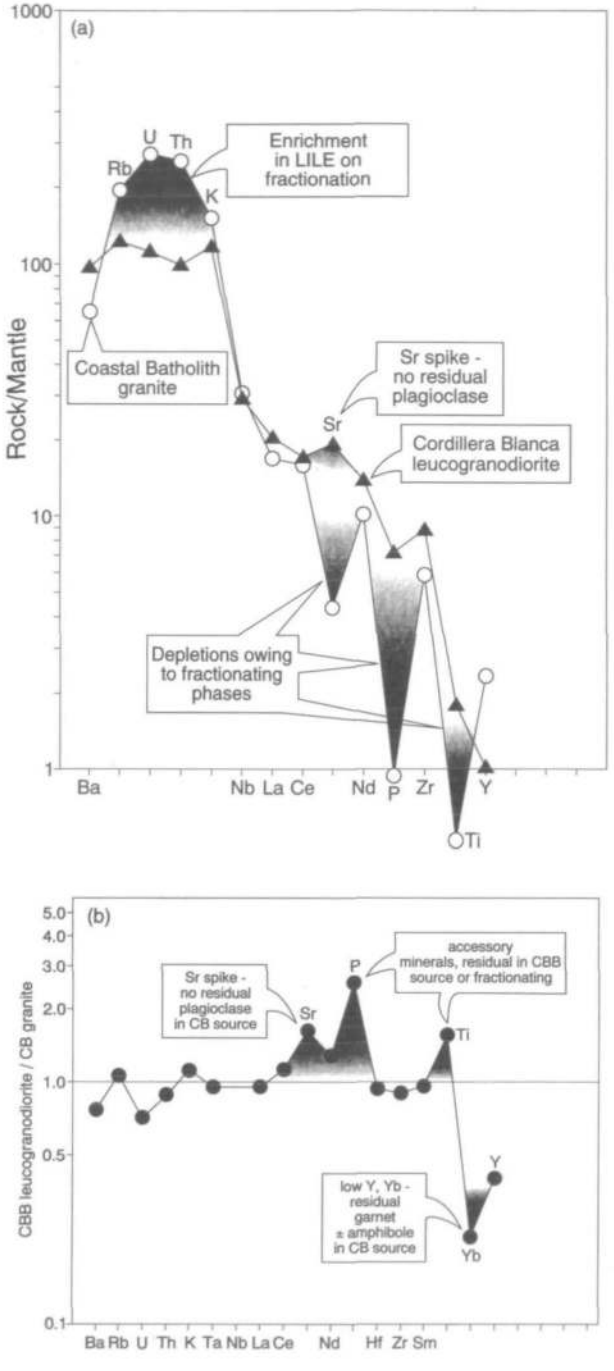

Fig. 13. (a) Mantle-normalized trace element diagrams of a leucogranodiorite (~72% SiO_2) from the Cordillera Blanca Batholith compared with a granitic rock (~72% SiO_2) from the Coastal Batholith, which was produced by crystal fractionation. The lack of LILE enrichment and major depletions in Sr, P and Ti in the Cordillera Blanca rocks is in contrast to the granitic rock of the Coastal Batholith, which evolved by early precipitation (fractionation) of plagioclase, apatite and titaniferous magnetite. (b) Incompatible element enrichment factors of a Cordillera Blanca Batholith leucogranodiorite compared with a Coastal Batholith granitic rock with similar SiO_2 contents (70% and 72%) and mineral assemblages.

coexisting quartz and its whole rock (Table 3). The pegmatite (92) has elevated $\delta^{18}O$ values by ~1‰ compared with the batholith rocks, consistent with the permitted maximum isotopic shift associated with magmatic fraction in hydrous granitic melts (O'Neil, 1986).

Although the data from the fault traverse are limited, they differ from other studies where deformation and subsequent resetting of oxygen isotope ratios led to higher $\delta^{18}O$ values in the most deformed rocks (Cartwright *et al.*, 1993). The general reduction in $\delta^{18}O$ values in the batholith rocks towards the faulted margin of the batholith may reflect limited interaction between the leucogranodiorites and low $\delta^{18}O$ meteoric fluids either during or after emplacement (e.g. Taylor, 1986). This interpretation is supported by the higher quartz and biotite values in the pegmatite and Yungay ignimbrite that lie to the west of the fault zone and an identical whole-rock value of +9·2‰ for the Yungay ignimbrite and the least deformed leucogranodiorite. Further evidence for interaction between the batholith rocks and low $\delta^{18}O$ meteoric–hydrothermal fluids are seen in the low $\delta^{18}O$ whole-rock values of +2·3‰ in a sheared xenolith and +4·1‰ in a leucogranodiorite from near the roof of the batholith (Table 3). Similar values characterize meteoric–hydrothermally altered volcanic roof rocks from the Yellowstone caldera (Hildreth *et al.*, 1984).

Equilibration temperatures calculated for mineral pairs (O'Neil, 1986), are also shown in Fig. 14 for the Cordillera Blanca rocks. Highest estimated temperatures of ~950°C occur in the Yungay ignimbrite, with the pegmatite giving a lower value of ~740°C. The high temperature in the Yungay ignimbrite places an important constraint on the emplacement temperature of the Cordillera Blanca batholith magmas. Unfortunately, owing to its fine grain size, no equilibration temperatures based on mineral pairs could be determined for the most deformed batholith rock (cataclasite). However, the subsolidus equilibration temperatures for the undeformed and deformed and partially recrystallized leucogranodiorites in the batholith (560–600°C) overlap, supporting earlier suggestions based on field and textural evidence that most of the deformation seen in the batholith rocks occurred during and shortly after emplacement (Petford & Atherton, 1992).

Although the oxygen isotopic composition of mantle-derived underplate remains obscure, it is notable that the range in primary (unaltered) whole-rock values for the Cordillera Blanca batholith rocks overlaps with the majority of $^{18}O/^{16}O$ values reported from the western Peninsular Ranges Bath-

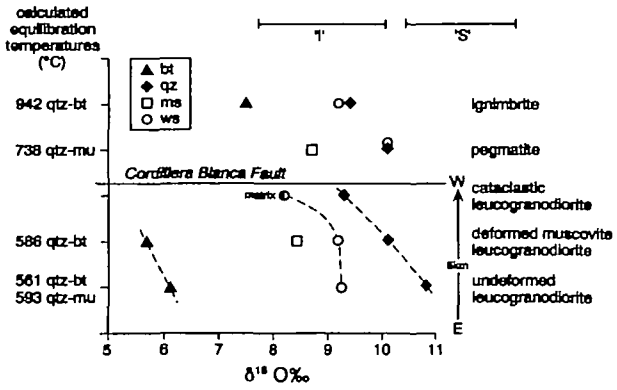

Fig. 14. δ^{18}O‰ data for minerals and whole rocks from the Cordillera Blanca. In the lower part of the diagram, the rocks are from a 5 km traverse from the undeformed leucogranodiorite at the centre of the batholith westwards to the cataclasite near to the western fault. The pegmatite and ignimbrite are exposed to the west. δ^{18}O‰ ranges for 'I' and 'S' type granitic rocks are after Taylor (1986). The matrix δ^{18}O‰ is shown for the cataclastic leucogranodiorite.

olith considered to have formed from partial melting of a meta-igneous crustal source, probably eclogite facies basaltic material (Taylor, 1986). Although the oxygen isotope ratios in the more acid Cordillera Blanca batholith rocks may well be due to limited assimilation of metasedimentary crust (see also radiogenic isotope section), similar $^{18}O/^{16}O$ (and $^{87}Sr/^{86}Sr$) ratios in granitic rocks of the eastern Peninsular Ranges Batholith are attributed mainly to changes in composition of the source region during partial melting of hydrated basaltic material (Taylor, 1986). Thus, relatively high δ^{18}O magmas may be produced directly from altered basic (lower-crustal) rocks during partial melting without recourse to extensive mid–upper-crustal assimilation. Certainly, the large difference in δ^{18}O values ($\sim +6$‰) between the high δ^{18}O Chicama shales means that, unlike many central Andean volcanic zone rocks, the batholith magmas have not interacted in a major way either with adjacent country rock or similar high $^{18}O/^{16}O$ material (Davidson *et al.*, 1991) at the level of emplacement.

PERALUMINOSITY, THE 'S' TYPE STATUS AND THE RELEVANCE OF THE 'THICK–THIN' MODEL TO THE DERIVATION OF Na-RICH ROCKS OF THE BATHOLITH

The recognition of peraluminous granitic batholiths ('S' type) inboard of metaluminous batholiths ('I' type) as exemplified by the Mesozoic plutonic belts in the western USA, has led to a general model of I–S duality in Mesozoic Circum-Pacific plutonism (Miller & Bradfish, 1980; Pitcher, 1983). The change to an 'S' type character towards the continental interior was considered to reflect the melting of, or major contamination by, thick continental crust. Pitcher (1983) considered that the Cordillera Blanca Batholith was part of such a duality, i.e. was 'generally peraluminous ... approaching "S" type composition'.

More recently, a similar model had been put forward for continental volcanic 'arc' magmas in North Chile (McMillan *et al.*, 1993). Along-arc magmas traversing 'thick crust' have been shown to have an enriched composition, specifically in incompatible trace elements, compared with those traversing thin crust. This enrichment has been interpreted by workers in the Andes as a reflection of an increased continental crust component gained on traversing thicker crust (Hildreth & Moorbath, 1988; McMillan *et al.*, 1993). The presence of the Cordillera Blanca Batholith within thick (>50 km) crust inboard of the Coastal Batholith emplaced within thin (<25 km) crust (Atherton, 1990) allows a critical appraisal of the application of these models to plutonism in Peru.

Considering the 'I'–'S' model first, Fig. 8 shows A/CNK values for the batholith rocks (range 0·80–1·39, mean 0·996, $n=64$, SD = 0·10). Only 19 of the rocks analysed have A/CNK > 1·0 and only seven have a value >1·10. 'S' type granites have A/CNK values >1·1 (Chappell & White, 1974). Thus the Cordillera Blanca Batholith is no more peraluminous than 'I' type granites which lack peraluminous minerals, e.g. Coastal Batholith (Fig. 8). The peraluminous rocks (A/CNK > 1·0) are the deformed rocks of the western margin, most of which are muscovite bearing (Petford & Atherton, 1992).

Muscovite is secondary, and the primary mineral assemblage, including hornblende, magnetite and sphene, indicates that the deformed facies is a modified 'I' type (Chappell & Stephens, 1988). Lead isotope compositions for the undeformed rocks support this; they are nearly identical to the related metaluminous hornblende-bearing Surco Stock to the south which has an A/CNK ratio of 0·86, and which could not have originated in old continental crust. According to Mukasa (1984), the source was 'enriched' mantle or underplated lower crust (Fig. 11). Furthermore, δ^{18}O values of +4·1 to 9·5‰ (Fig. 14) support an igneous, 'I' type, modified source.

The general concept or model whereby remobilization of old continental crust progressively increases as the locus of magmatism moves inland, away from the trench, clearly does not apply to central Peru.

Table 3: Oxygen isotope data for Cordillera Blanca rocks

Sample	Mineral	$\delta^{18}O$ SMOW (‰)	Distance from fault (km)	Comments
879	Quartz	+10·8	5	Undeformed leucogranodiorite
	Biotite	+6·1		
	Muscovite	+8·4		
	Whole-rock	+9·2		
918	Quartz	+10·1	3	Partially deformed muscovite-bearing leucogranodiorite
	Biotite	+5·7		
	Whole-rock	+9·2		
921	Quartz	+9·3	0	Cataclastic leucogranodiorite
	matrix	+8·2		
889	Quartz	+9·4		Yungay ignimbrite to west of fault
	Biotite	+7·6		
	Whole-rock	+9·2		
92	Quartz	+10·1		Pegmatite cutting leucogranodiorite
	Muscovite	+8·7		
	Whole-rock	+10·1		
Whole-rock data				
Batholith rocks				
880 (L)		+8·8		
884 (L)		+4·1		
900 (L)		+8·1		
921 (L)		+8·7		
925 (L)		+9·2		
915 (L)		+9·2		
93 (L)		+8·5		
901 (QD)		+6·2		
920 (T)		+9·2		
916 (P)		+9·5		
Mean		+8·1±1·7		
Sediments				
891		+14·1		
892		+14·4		
893		+14·2		
895		+13·6		
98		+15·4		
Mean		+14·3±0·66		
Xenoliths				
912		+2·3		
913		+13·3		

Mineral oxygen isotope ratios were determined at the NERC Isotope Geosciences Laboratory (UK) following the oxygen liberation technique of Clayton & Mayeda (1963) but utilizing a ClF_3 reagent (Borthwick & Harmon, 1982). Oxygen yields were converted to CO_2 by reaction with a platinized graphite rod heated to 675°C by induction furnace and analysed on a Phoenix 390 mass spectrometer. Data are given as per mille (‰) derivations relative to SMOW (Standard Mean Ocean Water). Standard sample NBS28 gave an average $\delta^{18}O$ value of +9·63±0·14‰ (n=3, analyst R. Greenwood) during this study. Whole-rock samples determined at SURRC (analyst A. Boyce). L, leucogranodiorite; QD, quartz diorite; T, tonalite; P, pegmatite.

With regard to the thick–thin crust model at continental margins (McMillan *et al.*, 1993), direct comparison of the most basic (≡ parental) magmas in the two batholiths is not possible, as only the leucogranodiorite of the Cordillera Blanca Batholith formed after the main Miocene thickening, i.e. in thick crust. If incompatible trace element abundances of rocks with ~72% SiO_2, with similar assemblages and textures, and which probably evolved by similar processes from both batholiths are ratioed they should provide information about deep crustal or mantle processes. Incompatible trace elements are usually arranged in order of increasing compatibility with peridotite, and if the thick–thin crust model applied to the Peruvian sector, all incompatible elements in the Cordillera Blanca rocks would show enrichment, with the exception of Y and the HREE. In North Chile, enrichment in 'thick crust' lavas for elements from Ba to Ti is consistently near ×2 (McMillan *et al.*, 1993). In contrast, the Cordillera Blanca rocks, which also lie on thick crust, show no such enrichment relative to those of the Coastal batholith (Fig. 13) within thin crust (Atherton, 1990). The enrichment of Sr and depletion of the HREE and Y (Fig. 13) are source related, i.e. garnet ± amphibole and little or no plagioclase were present in the Cordillera Blanca source. The P and Ti peaks are due to either source retention or fractional crystallization in the production of the Coastal Batholith granitic magma.

GENESIS OF THE CORDILLERA BLANCA BATHOLITH MAGMAS

Chemical characteristics of the leucogranodiorites

These rocks form a coherent group from 70 to 74% SiO_2, having chemical characteristics very different from the Coastal Batholith granites (data in parentheses), which were derived by a three-stage process from a source in the mantle wedge (Atherton, 1990):

(1) low HREE, average Yb 0·36 (Yb_{CB} average 1·99);

(2) high La_N/Yb_N ratios, >20, no Eu anomaly or only a small negative or positive one (La_N/Yb_{NCB} <20, Eu anomalies common);

(3) high Sr, >300 p.p.m. and Sr/Y generally >40 (Sr_{CB} average 202; Sr/Y_{CB} average 12·4);

(4) Rb/Sr low to moderate, 0·18–0·59; average 0·29 (Rb/Sr_{CB} 0·2–2·5);

(5) low Y, <15 p.p.m. (Y_{CB}, average 17);

(6) low to moderate K/Rb ratios, <400 (K/Rb_{CB} 240–320);

(7) moderately low Ba/La, average 38·5, 26–54 (Ba/La_{CB} average 81, 34–115), Rb/La average 4·0, 3·3–6·4 (Rb/La_{CB} average 7·7; 5–11), K/La average 1169, 894–1603 (K/La_{CB} average 1859, 1136–2479);

(8) high Al_2O_3, ≥15% ($Al_2O_{3\,CB}$, average 14·6%);

(9) Na_2O >4·0%, average 4·31% (Na_2O_{CB}, average 3·95);

(10) MgO, FeO, TiO_2 and CaO low compared with the Coastal Batholith (see Fig. 6);

(11) low Sc, <4 p.p.m. (Sc_{CB} 4–8 p.p.m.); low V, <25 p.p.m. (V_{CB} 25–50 p.p.m.).

Many of these characteristics match those of volcanic rocks considered to be the product of slab melting (Stern *et al.*, 1984; Defant & Drummond, 1990; Drummond & Defant, 1990; Peacock *et al.*, 1994). A single term adakite has been used for such rocks. Compositions are also similar, particularly in trace element and REE content, to Archaean high-Al trondhjemites (see Drummond & Defant, 1990), which have also been ascribed to oceanic slab melting (Martin, 1986).

Chemical characteristics of the tonalites and granodiorites

The chemistry of the more basic rocks (<70% SiO_2) is less distinctive compared with equivalent rocks of the Coastal Batholith; many elements overlap, although CaO is lower and Na_2O higher, whereas Al_2O_3 is much the same. However, Sr concentrations are higher and Y and Yb values lower (Fig. 8).

Partial melting of a basaltic source

Partial melts of a deep (>40 km) basaltic source will have the high Sr/Y and La/Yb ratios and low Y and Yb contents seen in both the leucogranodiorites and the tonalites if both garnet and amphibole but not plagioclase are residual in the source. The presence of residual amphibole in the more basic magmas is indicated by the concave upward form of the REE pattern (Fig. 9) as well as the high Al_2O_3 and low to moderate Rb/Sr and K/Rb ratios. On an La_N/Yb_N vs Yb_N diagram (after Jahn *et al.*, 1984; Martin, 1986) the Cordillera Blanca rocks lie in the Archaean high-Al TTG (tonalite, trondhjemite, granodiorite) field (Fig. 15a), whereas on Sr/Y vs Y diagram (Fig. 15b) they plot in the Archaean high-Al TTG field. In contrast, the Coastal Batholith rocks lie entirely in the post-Archaean granite or island-arc ADR (andesite–dacite–rhyolite) field (Fig. 15c).

Trends produced by variable degrees of partial melting of basalt on La_N/Yb_N vs Yb_N (Fig. 15a) and

on Sr/Y vs Y (Fig. 15b) diagrams have been modelled (see Jahn *et al.*, 1984; Martin, 1986; Drummond & Defant, 1990). Source compositions vary from eclogite (qz/cpx/ga: 15/55/30) to amphibolite (hble/plag/bio: 70/25/5) with source REE patterns ranging from flat to slightly LREE enriched ($La_N/Yb_N = 4$). The La_N/Yb_N and Sr/Y plots (Fig. 15) suggest that leucogranodiorite melts could have formed from garnet amphibolite to eclogite sources, whereas most of the tonalites may have formed from a source with less garnet.

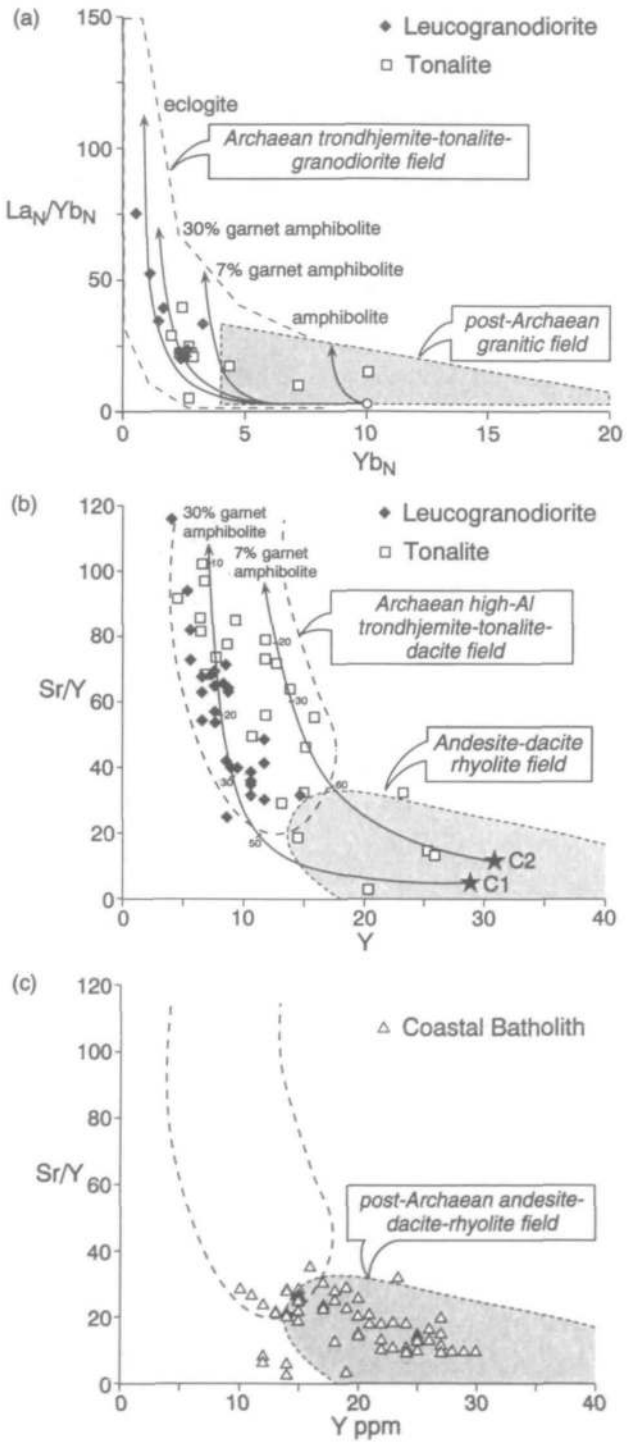

Fig. 15. (a) La_N/Yb_N vs Yb_N plot, showing Archaean trondhjemite–tonalite–granodiorite (TTG) and post-Archaean granitic fields (after Martin, 1986). It should be noted that the leucogranodiorites and most of the tonalites–diorites of the Cordillera Blanca lie in the Archaean field (TTG). Batch partial melting trends from a continental basalt source with mineralogies of eclogite, garnet-free amphibolite and amphibolite with 7% and 30% garnet are also shown. From this modelling, garnet-bearing amphibolite and possibly eclogite sources can account for the geochemical characteristics of the granitic rocks. Symbols as in Fig. 3. (b) Sr/Y vs Y plot of rocks from the Cordillera Blanca Batholith Fields after Drummond & Defant (1990). Melting curves were drawn using batch melting equations and the mineralogy determined from the REE modelling (see Fig. 18). C_1 and C_2 are two source compositions consistent with the REE, Sr and Y data. (c) Sr/Y vs Y plot of rocks from the Coastal Batholith (Lima segment). These rocks have low Sr/Y ratios and plot in the post-Archaean andesite–dacite–rhyolite field [equivalent to the granite field of Martin (1986)].

Continental crust vs slab source

The critical requirement of the sources of the tonalites and leucogranodiorites is that they contained garnet and amphibole (with little or no plagioclase) in the residue so that partial melts would be high-Al types with high La_N/Yb_N ratios and high Na_2O and Sr contents. There are two environments in which this might occur: (1) subducted oceanic lithosphere; (2) lower continental crust (thicker than 40 km). With regard to (1), Martin (1986) has maintained that Archaean and post-Archaean granitic rocks are significantly different; the former related to partial melts of a garnet–hornblende source whereas modern granitic rocks show no indication of a prominent role for either of these minerals. This he considers is a direct consequence of the progressive cooling of the Earth. Because Archaean oceanic crust was young and warm it melted before dehydration, leaving a garnet + hornblende residue. Modern oceanic crust of major ocean basins, being old (average 60 Ma) and cold, dehydrates before reaching the solidus of hydrated tholeiite, and so is subducted without melting (Peacock *et al.*, 1994). In this latter situation, it is the 'fluid metasomatized mantle wedge' above the slab that melts to produce the magmas, and olivine and pyroxene are the dominant residual phases.

Slab melting has also recently been put forward to explain a group of Cenozoic to Recent high-Al volcanic arc rocks with similar chemical characteristics to the leucogranodiorites, which are apparently restricted to sites similar to those in the Archaean where young (<25 Ma), hot oceanic plate subducts

(Defant & Drummond, 1990). The slab melting model is attractive with respect to the genesis of the Cordillera Blanca leucogranodiorites, as subduction has been a major feature of the continental margin since at least the Jurassic (Fukao *et al.*, 1989), and the rocks have characteristics apparently consistent with slab melts. However, geophysical, isotopic and age data and thermal modelling suggest that partial melting of a mafic protolith in the base of the thick crust (>40 km) beneath the batholith is more likely in this case [a brief discussion has been given by Atherton & Petford (1993)].

Here we discuss the two most compelling reasons why we consider that lower-crustal melting rather than slab melting produced the magmas of the Cordillera Blanca Batholith:

(1) Numerical modelling of pressure–temperature–time paths of subducting amphibolitic oceanic crust indicates that partial melting can only occur on subduction of very young (5–10 Ma) oceanic lithosphere (Peacock *et al.*, 1994). Alternatively, with high rates of shear heating, shear stresses $\geqslant$100 MPa must be maintained by rocks close to their melting temperature to cause partial melting. This we consider to be implausible, and so the age of the subducting slab becomes critical. As the Nazca plate at 20–5 Ma was not at the initial stage of subduction and was 55 to 65 Ma at the trench (Wortel, 1984), it was clearly too old and cold for melting to occur before dehydration.

(2) The thermal structure in subduction zones has been much studied, with slab-induced convection an important aspect of the models (Peacock, 1991; Davies & Bickle, 1991). Local high temperature gradients are produced along the slab–wedge interface. Various assumptions as to the slab subduction angle, etc. place slab melting, if it occurs, in the corner of the mantle wedge at ~60–70 km depth (Peacock *et al.*, 1994) but importantly some 80 km from the trench, outboard of the main plutonic–volcanic arc, i.e. in the arc–trench gap (Fig. 16, and Davies & Stevenson, 1992). In Peru, the reverse is the case, the Cordillera Blanca Batholith lying ~300 km inboard of the trench and the volcanic 'arc' and directly above the thickened keel of the Andes. Such a geometry is more consistent with derivation from hot, newly thickened basaltic crust beneath the batholith, but not from the subducted slab.

REE modelling of the batholith

We present here a two-stage model that relates the generation of the Cordillera Blanca batholith to the dynamic underplating of the Andean crust during Miocene times. Stage 1 involves the creation of a mafic underplate by partial melting of slightly enriched upper mantle. In stage 2 this newly accreted material is itself partially melted, giving rise to the older tonalites and, later after the underplate has thickened through the garnet-in transition, the more voluminous leucogranodiorites. Thus the evolution of the batholith dynamically 'mirrors' the thickening, and formation of the keel of the Andes in central Peru.

Stage 1: Generation of the mafic crustal underplate

In the modelling we use a late high-Al, calc-alkaline basaltic dyke rock (Table 1) from the Cordillera Blanca with an La_N/Yb_N value of near four as a guide to the composition of the accreted material that might form the deep crustal keel. This rock is similar to the Eocene–Miocene (14·6 Ma) calc-alkaline basalts immediately to the west of the Cordillera Blanca fault (Fig. 1), which have values near four (Atherton *et al.*, 1985, table 25.2).

There are two possible sources for basalt magma, both of which may occur in the subcontinental lithosphere depending on depth: spinel or garnet (±spinel) peridotite. Xenoliths of both types have REE patterns which are not very dissimilar (McDonough & Frey, 1989). Anhydrous fertile peridotites with high Al_2O_3 and CaO contents tend to have La_N/Yb_N ratios near unity or less, whereas infertile mantle types with low values of these oxides owing to basalt extraction often have enhanced LREE, indicating a later, separate enrichment event (McDonough & Frey, 1989).

Two end-member type mantle compositions from McDonough & Frey (1989) were used in the modelling (Fig. 17): an infertile garnet peridotite xenolith, with a relatively steep REE pattern (La_N/Yb_N value of 40) and a fertile garnet peridotite xenolith with an La_N/Yb_N ratio of just over two.

No partial melts (F values 0·01–0·2) could be produced from infertile mantle which approximates the REE pattern of the late basalt. However, partial melting (7–10%) of the fertile mantle source could produce a melt similar to the basalt (Fig. 17), and this was tested as a probable basalt source in modelling partial melting giving rise to the quartz diorite–tonalite and the leucogranodiorite.

Stage 2: Generation of batholith magmas

From previous discussions on field and age constraints, and from the observed trace element and REE profiles of the batholith rocks, any proposed model for their origin must account for the following:

(1) The quartz diorites and tonalites are older

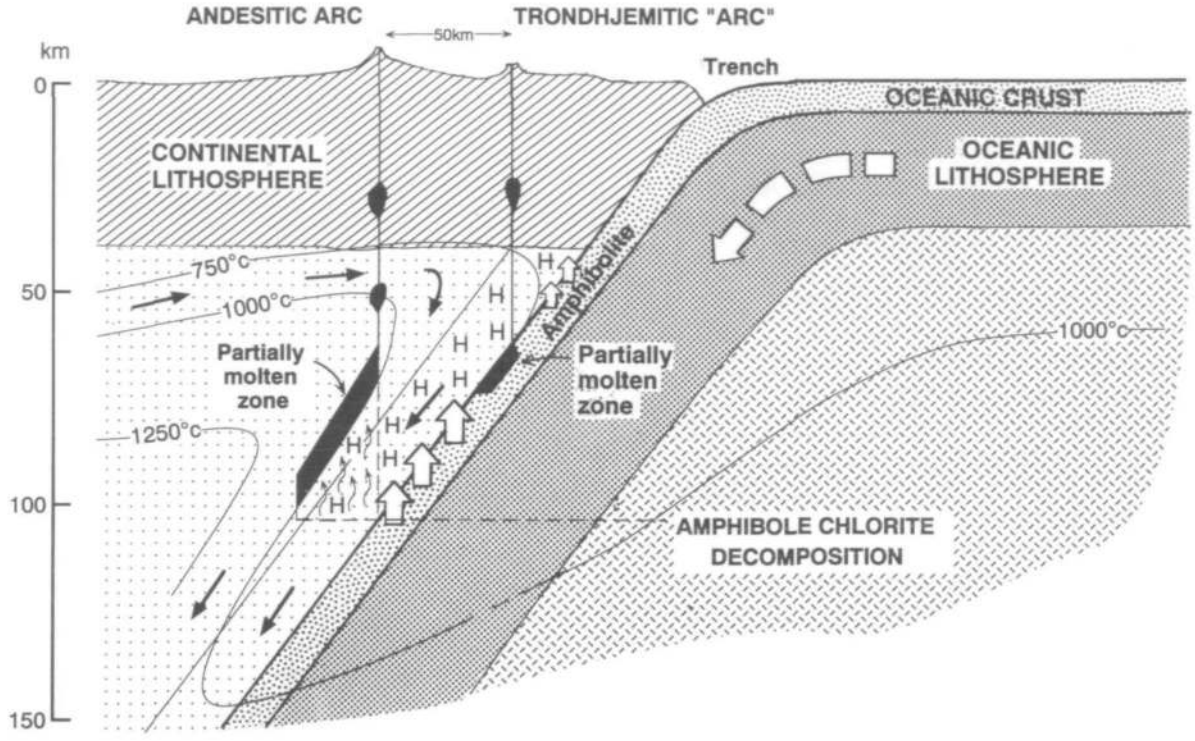

Fig. 16. Diagram showing subduction zone geometry at a continental margin, illustrating the relative positions of a trondhjemite to a tonalite (or andesitic) 'arc'. Fluid-absent melting of oceanic lithosphere can only occur during subduction of very young (<5 Ma) oceanic crust (Peacock *et al.*, 1994) at temperatures near 750°C and pressures <2 GPa. This places the melting zone near the intersection of the top of the slab with the 750°C isotherm. In contrast, hydrated peridotite formed by addition of slab-derived H_2O is dragged down to near 110 km where amphibole and chlorite in a peridotite system break down through nearly pressure-dependent reactions (Tatsumi, 1989). It should be noted that amphibole is stable in mantle peridotite at higher P–T conditions than in the basalt system (Tatsumi, 1989). H_2O percolates up through the 1000°C geotherm, the solidus temperature of peridotite under the H_2O-saturated conditions where partial melting occurs. From these mantle wedge magmas tonalitic rocks of most Cordilleran calc-alkali suites are ultimately produced (see Davies & Stevenson, 1992). This relative positioning of the Na-rich arc nearer to the trench is the opposite to that in Peru, where the Cordillera Blanca Batholith Na-rich rocks are the youngest and most easterly manifestation of Andean magmatism, some 300 km from the trench.

than the leucogranodiorites, and are separated by a plutonic hiatus of ~8 Ma.

(2) The more basic nature of the early quartz diorite–tonalite facies requires a higher degree of partial melting in the mafic source region than for the younger, more acidic leucogranodiorites.

(3) The steepening La_N/Yb_N ratios from the quartz diorite–tonalite to the leucogranodiorites (Fig. 9) requires more garnet in the leucogranodioritic source region, suggesting that the crust thickened through the garnet-in transition after the generation of the more basic melts (Atherton & Petford, 1993).

(4) The LREE contents of the leucogranodiorites are similar to or lower than those of the tonalites and diorites. Smaller degrees of partial melting of the same source would, however, produce greater LREE enrichment in the leucogranodiorites than in the tonalites. It follows that their source must have been less enriched in LREE, or a change in the residual mineralogy may have been responsible.

(5) High Sr contents in both facies and Sr/Y modelling requires low plagioclase content in the source (<10%) or a more albitic plagioclase which would retain little Sr.

Tonalites and quartz diorites

The first melts from the underplate are the older quartz diorites, and tonalites, e.g. 901 and 68 with 55% and 63% SiO_2, respectively. These can be modelled by relatively high degrees of partial melting of the underplated basalt (33–40%) producing melts with low La_N/Yb_N ratios (28·8–21). Residues include amphibole, clinopyroxene and low to moderate amounts of garnet (Fig. 18). For simplification, data in the summary diagram (Fig. 18) refer to an average diorite (901) only.

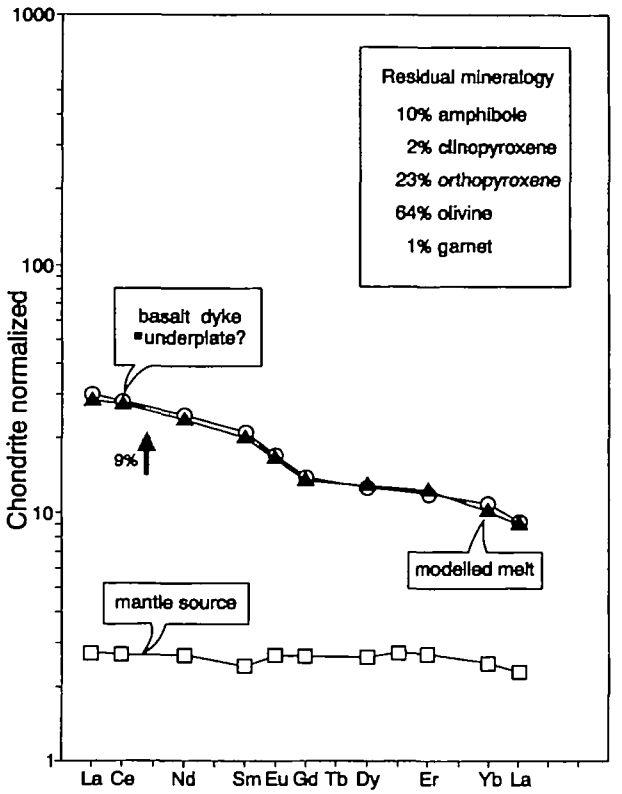

Fig. 17. Mantle melting model for the generation of the underplate involves 9% batch melting of an enriched (×2·5) hydrous fertile mantle source similar to that proposed by Lopez-Escobar *et al.* (1979) as a source for the central Chile granitic rocks. This produces a melt similar in composition to the Cordillera Blanca basaltic andesite 86, and similar to late dykes in the Eocene–Miocene lavas to the west. Mantle K_D values are from Martin (1986), after Hanson (1980). Residual mineralogy is similar to that seen in mantle xenoliths from the Sierra Nevada Batholith (Bateman, 1992), and expected after large-scale hydration of the lithosphere above subducting slabs (Peacock, 1993).

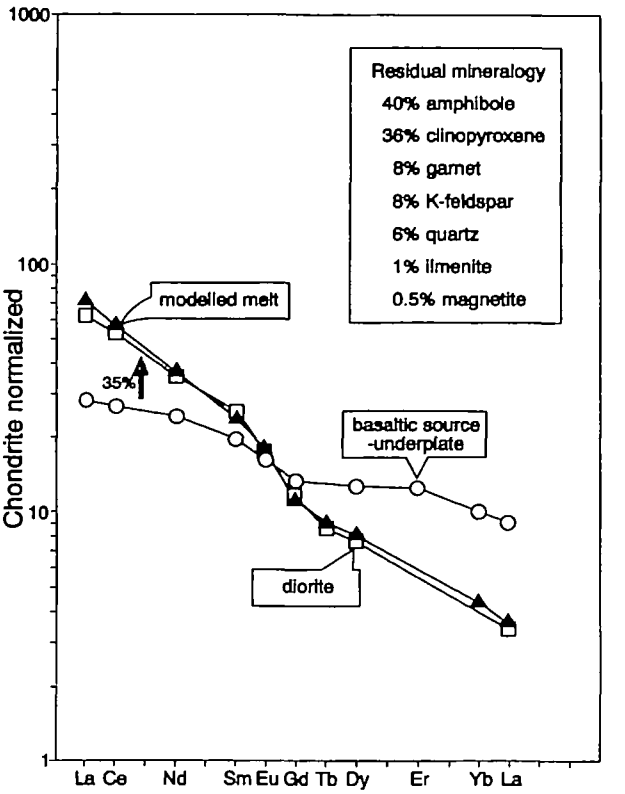

Fig. 18. Batch melting model of garnet amphibolite basaltic underplate to produce a typical tonalite. Melt proportions and residual phases are comparable with the experimental partial melts of amphibolite–eclogite, giving tonalitic melts at 16 kbar (Rapp *et al.*, 1991) although residual amphibole here is higher and garnet lower in amount. [See also the experimental data of Sen & Dunn (1994) at 1·5 GPa, where residual amphibole is similar in amount.] Mineral–melt distribution coefficients for plagioclase, garnet, amphibole, clinopyroxene, magnetite and ilmenite from the compilation of Martin (1987); quartz and K-feldspar from Nash & Crecraft (1985).

Leucogranodiorites

As the leucogranodiorites have LREE similar to, or lower than, the tonalites and diorites (Fig. 9), lower degrees of partial melting of the same source produced model liquid compositions with LREE enrichments far greater than those observed. Changes in melt fraction have little effect. Neither does the source mineralogy, as lower-crustal LREE K_D values for clinopyroxene and garnet are not very different, so the change from a dominantly clinopyroxene (+amphibole) to a dominantly garnet (+amphibole+clinopyroxene) residue as indicated in the Sr/Y vs Y modelling should not significantly reduce the LREE enrichment for smaller partial melts. The LREE abundances in the source region must therefore be lower than those of the older tonalites. Furthermore, the lower HREE abundances in the leucogranodiorites indicate more residual garnet in the source. Thus, the leucogranodiorite can be modelled by 16–20% partial melting of a mafic source slightly depleted in LREE, relative to the source of the older tonalites, leaving residues of 35 and 25% garnet, plus amphibole and clinopyroxene. Modelled profiles are similar to those of the two rocks defining the envelope of the leucogranodiorites (see Fig. 9). For simplification, the summary diagram (Fig. 19) refers to the most evolved leucogranodiorite. The residual mineralogy is compatible with the Sr/Y modelling and is not very different from the results of Martin (1987) for similar Archaean high-Na rocks from Finland.

On an Sr/Y vs Y (Fig. 15b) the tonalites–quartz diorites lie to the right of the leucogranodiorites with a very similar range in Sr/Y ratios but higher Y values. Modelling of partial melting trends clearly

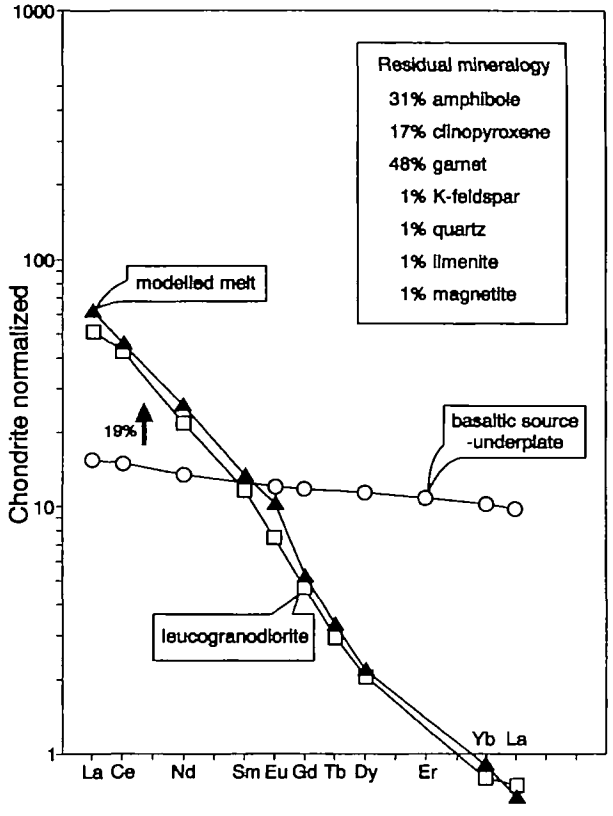

Fig. 19. Batch melting model of garnet amphibolite underplate to produce the most HREE depleted leucogranodiorite. Melt proportions and residual phases are comparable with experimental partial melts of amphibolitic eclogite which are Na rich at ⩾16 kbar (Rapp *et al.* 1991) although, again, the more hydrous nature of the residue means amphibole exceeds clinopyroxene. [See Sen & Dunn (1994) for experimental data on amphibole-rich residues.] Mineral–melt distribution coefficients as in Fig. 19.

shows this relates to sources with higher Sr contents than those of the leucogranodiorite (Fig. 15b). Using the parameters determined from the REE modelling and the Sr and Y data, the source of the tonalites–quartz diorites had an Sr content of 351–364 p.p.m. and a Y content of 25–31 p.p.m., whereas the leucogranodiorite source had an Sr content of 99–132 p.p.m. and a Y content of 26–30 p.p.m.

EXPERIMENTAL STUDIES

As interstitial pore fluid is unlikely to be present in the lower crust, partial melting is considered to occur in fluid-absent conditions. Consequently, experimental studies, post-1990, have concentrated on the melting behaviour of hydrous rocks across a broad range of temperature and fluid saturation at pressures equivalent to the lower crust or deeper in subducted slab. Low melt fraction liquid compositions relevant to the Cordillera Blanca magmas have been determined for amphibolite, garnet amphibolite and eclogite sources (Beard & Lofgren, 1991; Rapp *et al.*, 1991; Van der Laan & Wyllie, 1992; Rushmer, 1993; Sen & Dunn, 1994; Rapp & Watson, 1995). Thus partial melting of mafic crust with the mineralogies given above has been proposed as a common mechanism for the large-scale production of tonalitic continental crust magmas, as well as the high-Na magmas (TTG) of the Archaean. These magmas can be distinguished from post-Archaean magmas by their strongly fractionated REE patterns and depleted HREE (Martin, 1987), reflecting the presence of garnet and/or amphibole as important residual phases in the source (Arth *et al.*, 1978). The liquids produced in the experiments are broadly similar to Archaean TTG rocks and some more recent 'arc' magmas including those of the Cordillera Blanca (Fig. 5, Sen & Dunn, 1994; Rapp & Watson, 1995). Residues formed during the experimental studies for fluid-absent melting and water-undersaturated melting to 1·2 GPa include amphibole, clinopyroxene, garnet and plagioclase. These are similar to assemblages found in lower-crustal xenoliths from a variety of areas (Toft *et al.*, 1989; Rushmer, 1993; Rapp & Watson, 1995). Partial melting of such mafic rocks occurs by a few important peritectic reactions (Rapp & Waton, 1995). Garnet forms by the breakdown of amphibole plus plagioclase under fluid absent conditions at pressures of 12–18 kbar:

$$\text{amph} + \text{plag} \pm \text{qtz} = \text{garnet} + \text{cpx} + \text{melt} + \text{new plagioclase (albitic)}.$$

At the bulk compositions of these experiments (Rushmer, 1993) amphibole remains stable with garnet up to at least 15 kbar. At higher pressure (up to ~22 kbar) plagioclase and amphibole are destabilized as garnet and clinopyroxene are stabilized to eclogitic assemblages. The presence of garnet in the experimental studies at pressures from 12 to 18 kbar has a major impact on melt composition, causing an increase of Si and decrease in Fe, Mg, Ti and Ca, and the production of a high-Al type character (Rushmer, 1993). These are precisely the characteristics noted in the leucogranodiorites of the Cordillera Blanca Batholith compared with equivalent rocks of the Coastal Batholith (Fig. 6), where the mafic parental magmas were generated by partial melting of spinel peridotite within the mantle wedge (Atherton & Sanderson, 1985). For less acidic compositions (<70% SiO_2) these rather subtle distinctions are less clear, indicating that the leucogranite magmas mark the incoming of significant residual garnet in the source.

GEOPHYSICAL CONSEQUENCES OF REE MODELLING

Using the mineral proportions of the residues obtained from the REE modelling, it is possible to estimate the physical properties of the source of the Cordillera Blanca magmas, and to compare these estimates with measured geophysical properties of the lower crust. The residues for both quartz diorites–tonalites and leucogranodiorites are made up mostly of clinopyroxene, amphibole and garnet, in varying proportions with minor quartz and feldspar (Figs 18 and 19). Estimated densities [using pressure corrected values from Christensen (1982)] of the solid residues range from $\sim$2·95 g/cm^3 for the tonalite source to 3·01 g/cm^3 for the leucogranodiorite source, the latter (higher) value reflecting the greater amount of garnet. These values are close to the measured value of 3·0 g/cm^3 for the mid to lower crust (James, 1971; Fukao *et al.*, 1989, and Fig. 2). The seismic velocity of the residue can be estimated from measured P- and S-wave velocities for individual minerals (Toft *et al.*, 1989; Rushmer, 1993). When expressed in terms of Poisson's ratio, our estimated values of 0·26 for the quartz diorite–tonalite residue and 0·27 for the leucogranodiorite residue compare favourably with measured lower-crustal values of $\sim$0·29 (James, 1971).

Seismic velocities (V_p) of mantle-derived mafic underplate have been estimated at between 7·0 and 8·1 km/s, depending upon chemical composition and thermal structure (Furlong & Fountain, 1986). The relatively low measured P-wave velocities beneath central–northern Peru of between $\sim$6·5 and 7·0 km/s (James, 1971) support the earlier proposition of crust that is mafic, relatively dense and very hot.

DISCUSSION

In our model for the evolution of the magmas of the Cordillera Blanca Batholith the source changed with time from that producing the early quartz diorites and tonalites of the western and southern margins (14–10 Ma) to one producing the leucogranodiorites at $\sim$6–5 Ma. The later magmas left residues with more garnet than the earlier magmas, indicating that the source deepened over this period and the well-documented rapid uplift over the period 26–5 Ma (with very rapid uplift from 14 to 5 Ma; Sebrier *et al.*, 1988) was caused by the crustal thickening over this period. Thus the intrusion of the batholith closely followed crustal thickening. Kono *et al.* (1989), from geophysical and geological evidence, considered that the crustal thickening in the Western Cordillera was essentially by magmatic addition. Their model, which contains elements of earlier models, e.g. those of James (1971) and Suarez *et al.* (1983), envisaged a partitioning of the deformation so that tectonic thickening dominated in the Eastern Cordillera, whereas magma accretion dominated in the Western Cordillera. However, magmatism was not confined to the western Andes, as shown by the extensive volcanism across the Altiplano. A similar continuous, dual model for crustal thickening for the South Central Andes ($\sim$21°S) has recently been put forward by Schmitz (1994).

Over the period 26–6 Ma plate convergence was shallow (10–30°) and fast, $\sim$10 cm/yr (Pilger, 1984). This would generate magma across a wide zone from a mantle which was undergoing marked secondary convection and large-scale hydration producing amphibole, etc. (Tatsumi, 1989; Peacock, 1993). This is important in replenishment of the mantle wedge (Thorpe *et al.*, 1981) as well as promoting partial melting (Davies & Bickle, 1991). Such a process could also be effective in transporting lithospheric material from the internal parts of the continent. Kono *et al.* (1989) considered that magma generated under these conditions was responsible for the crustal thickening.

The amount of material needed to produce the thickening over the period 25–5 Ma by this method alone is large (see Kono *et al.*, 1989; Petford *et al.*, 1996). However, two aspects of the problem are relevant. First, assessments of the magmatic addition to crust have commonly used volumes of volcanic and plutonic rocks seen at the surface [see Kono *et al.* (1989) for a review]. This is likely to be an underestimate, and could be grossly wrong if we consider that mantle-derived magmas may well be arrested at major density interfaces, especially at convergent margins (Herzberg *et al.*, 1983). Indeed, the notable absence of any basaltic–andesitic syn- or late-plutonic dykes (in contrast to the Coastal Batholith) and the large, essentially granitic batholith, as well as the strong Oligo-Miocene volcanism (Sebrier *et al.*, 1988) associated with MASH (melting, assimilation, storage, homogenization; Hildreth & Moorbath, 1988) processes at depth have been used to infer, from thermal arguments, major basalt stalling in the deep crust.

Second, there is strong evidence today for the anomalous thermal state of the crust in Peru. A striking feature of the James (1971) model is the low shear velocity in the upper mantle beneath the Andes (4·25–4·30 km/s). Hot upper mantle in this zone is in accordance with the high electrical conductivity zone (0·1 S/m) following the mountain range just to the south of the Cordillera Blanca

(Schmucker, 1969). It lies ~50 km below the present surface and may be correlated with a low-velocity zone (Ocola & Meyer, 1972) below 40 km. Conductivity values are similar to those in the Basin and Range province of North America, which Bott (1982) thought likely to be a melt fraction in highly conducting rock. Aqueous fluids are ruled out at these depths. A hot crust above the hot upper mantle is indicated by the high heat flow measurements across this zone and the Altiplano (40–60°C/km, Uyeda & Watanabe, 1970), and active thermal springs along the line of the Cordillera Blanca fault system.

The conjunction of rapid uplift, extension, rapid heating of the lower crust, increased magmatism over the period 26–5 Ma and the extensional collapse is consistent with some form of delamination or 'catastrophic' mechanical thinning of the lithosphere beneath the Western Cordillera [see Dewey (1988), who considered only three places world wide, of which the Andes is one, where delamination is occurring]. It is also consistent with the undefined Moho in the Western Cordillera further south at 21–24°S (Schmitz, 1994). Isostatic uplift is generated when hot, less dense asthenosphere replaces cold, dense lithosphere. This results in basaltic accretion in the lower crust generated by decompression partial melting of asthenosphere (Nelson, 1992), followed by considerable lower-crustal fluid-absent melting. Under such lithospheric regimes up to 25 km of basaltic material may be accreted, by underplating, to the crust (Furlong & Fountain, 1986). In the region northeast of Lima, where the crust is ~55 km thick, the magmatic addition would be ~20 km, assuming a pre-26 Ma crust of 35 km.

According to Pilger (1984) and Wortel (1984), slab dip in Northern Peru progressively shallowed from ~30° at ~25 Ma to 10° today. This would account for the lithospheric erosion indicated by the uplift, etc. Melts from a dynamically thickening crust should show a sequence indicating the incoming of garnet and the disappearance of plagioclase as a residual phase. Diagnostic trace element signatures of delamination-related magmas in thick continental crust (Kay & Kay, 1991), high La_N/Yb_N and Sr/Y ratios, and the lack of a negative Eu anomaly mirror this process and are characteristic of the rocks of the Cordillera Blanca.

Thus we envisage that the dynamic evolution of magma type relates to the building of the thick crustal keel. Underplated mafic magmas from ~25 Ma or earlier produced the proto keel of the Western Andes. Continued accretion, possibly with a component of magmatic over-accretion, i.e. magma piercing the Moho to form a layered lower crust, would displace the new root down through garnet-in to finally produce the garnetiferous rocks at pressures at depths of >40 km, at the base of the crust. Over the period 19–3 Ma major plate movement occurred, which produced strike slip, transtensional structures of crustal dimensions, i.e. the Cordillera Blanca fault system (Petford & Atherton, 1992), which tapped basic magmas at 14 Ma and ~10–9 Ma, and finally Na-rich granitic magmas at ~6–5 Ma in the thickened, garnetiferous deep crust (>50 km) (Fig. 20). In this model we envisage little residence time of the basaltic material in the crust before partial melting. This is compatible with the isotopic data, which are indistinguishable from the mantle reservoir defined by Tilton & Barreiro (1980) in central Chile.

The rocks of the Cordillera Blanca are in many respects similar to Archaean trondhjemites, but we maintain here that the source is not subducted ocean crust as suggested by Martin (1987). Magmas with apparent 'Archaean' chemical signatures can be produced in a post-Archaean setting in deep crust (~50 km) where garnet and amphibole are stable. Thus in Peru Na-rich rocks of the Cordillera Blanca Batholith occur over thick crust and inboard of the more common tonalite–granodiorite–granite suites of the Coastal Batholith lying over thin crust. The magmas formed from newly underplated material by a multistage process which involved the production of hydrous basalt from the hydrated mantle wedge (Peacock, 1993), which was quickly melted after the formation of an underplate to form the Cordillera Blanca Na-rich suite. The Cordillera Blanca Batholith is not 'S' type as previously suggested; peraluminosity is slight and related to high-level deformation. It is a modified 'I' type and differs in chemistry, isotopic composition and proportion of acid (>70% SiO_2) material from the Coastal Batholith, which lies nearer the continental margin. Simplified models of granitic belts are not useful in modelling circum-Pacific belt magmatism. Sources may be in 'thick' or 'thin' crust and vary in time as well as in space, laterally and longitudinally within the Andean belt. Continental margin batholiths are dynamically related to major crustal events such as rifting in the case of the Coastal Batholith (Atherton, 1990) or magmatic accretion and uplift in the case of the Cordillera Blanca. There is no simple, common pattern at Pacific continental margins.

ACKNOWLEDGEMENTS

We thank Marge Wilson and Andrew Saunders for thorough, thoughtful, incisive reviews. We are

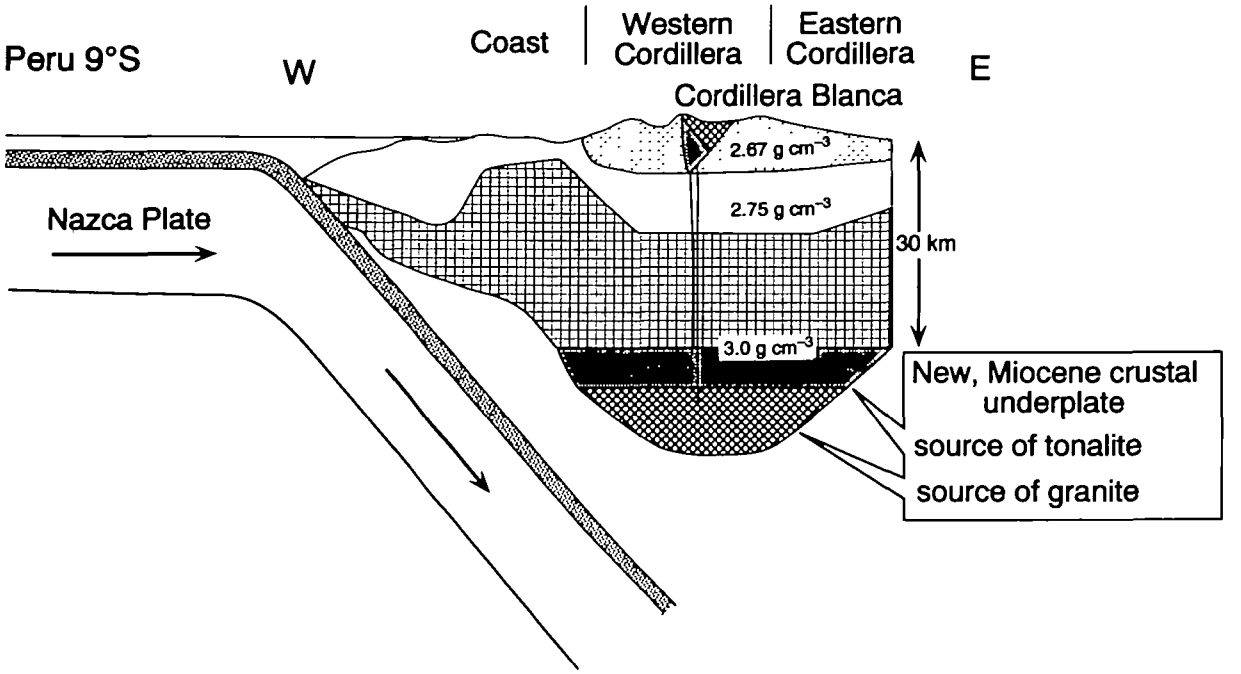

Fig. 20. Schematic representation of the crustal evolution in the region of the Cordillera Blanca Batholith near 9°S during late Miocene times based on the geophysical data of Couch *et al.* (1981), who defined a three-layer crust. Crustal thickening and uplift was at a maximum during the period 15–3 Ma [see Kono *et al.* (1989) for a review], coinciding with the emplacement of the Cordillera Blanca batholith, whose source is this newly thickened crust made of hydrated basalt. The existence of a mafic underplate is consistent with geophysical and geochemical data. Major tectonic thickening was confined to the eastern Andes (Kono *et al.*, 1989). The scheme shows that the crust thickens with time and thus that the source of the magmas becomes deeper, such that the tonalitic melts were generated at lower pressures than the later leucogranodioritic melts, which formed from a more garnet-rich source.

grateful to Alex Halliday, Barbara Barreiro and Richard Greenwood for providing support in radiogenic and stable isotopic analysis, to Helen Orme for the modelling, and Kay Lancaster for most of the draughting. Special thanks are due to Marge Wilson for patient and encouraging support. The errors still remaining are, of course, ours.

REFERENCES

Arth, J. G., Barker, F., Peterman, Z. E. & Friedman, I., 1978. Geochemistry of the gabbro–diorite–tonalite trondhjemite suite of southwest Finland and its implications for the origin of tonalitic and trondhjemitic magmas. *Journal of Petrology* **19**, 289–316.

Atherton, M. P., 1984. The Coastal Batholith of Peru. In: Harmon, R. S. & Barreiro, B. A. (eds) *Andean Magmatism: Chemical and Isotopic Constraints*. Nantwich, UK: Shiva, pp. 168–179.

Atherton, M. P., 1990. The Coastal Batholith of Peru: the product of rapid recycling of new crust formed within rifted continental margin. *Geological Journal* **25**, 337–349.

Atherton, M. P., 1993. Granite magmatism. Celebration Paper. *Journal of the Geological Society of London* **150**, 1009–1023.

Atherton, M. P. & Petford, N., 1993. Generation of sodium-rich magmas from newly underplated basaltic crust. *Nature* **362**, 144–146.

Atherton, M. P. & Plant, J., 1985. High heat production granites and the evolution of Andean and Caledonian continental margins. *Institute of Mining and Metallurgy*, 459–479.

Atherton, M. P. & Sanderson, L. M., 1985. The chemical variation and evolution of the superunits of the segmented Coastal Batholith. In: Pitcher, W. S., Atherton, M. P., Cobbing, E. J. & Beckinsale, R. D. (eds) *Magmatism at a Plate Edge: the Peruvian Andes*. Glasgow: Blackie Halstead Press, pp. 207–228.

Atherton, M. P. & Sanderson, L. M., 1987. The Cordillera Blanca Batholith: a study of granite intrusion and the relation of crustal thickening to peraluminosity. *Geologische Rundschau* **76**, 213–232.

Atherton, M. P., Sanderson, L. M., Warden, V. & McCourt, W. J., 1985. The volcanic cover: chemical composition and the origin of the magmas of the Calipuy Group. In: Pitcher, W. S., Atherton, M. P., Cobbing, E. J. & Beckinsale, R. D. (eds) *Magmatism at a Plate Edge: the Peruvian Andes*. Glasgow: Blackie Halstead Press, pp. 273–284.

Bateman, P., 1992. Plutonism in the central part of the Sierra Nevada Batholith, California. *US Geological Survey Professional Paper* **1483**, 186 pp.

Beard, J. S. & Lofgren, G. E., 1991. Dehydration melting and water saturated melting of basaltic and andesitic greenstones and amphibolites at 1·3 and 6·9 kbar. *Journal of Petrology* **32**, 365–401.

Beckinsale, R. D., Sanchez-Fernandez, A. W., Brook, M., Cobbing, E. J., Taylor, W. P. & Moore, N. D., 1985. Rb–Sr whole rock isochron and K–Ar age determinations for the Coastal Batholith of Peru. In: Pitcher, W. S., Atherton, M. P., Cobbing, E. J. & Beckinsale, R. D. (eds) *Magmatism at a Plate*

Edge: the Peruvian Andes. Glasgow: Blackie Halstead Press, pp. 177–203.

Borthwick, J. & Harmon, R. S., 1982. A note regarding ClF_3 as an alternative to BrF_5 for oxygen isotope analysis. *Geochimica et Cosmochimica Acta* **46**, 1665–1668.

Bott, M. P. H., 1982. *The Interior of the Earth: its Structure, Constitution and Evolution*. London: Arnold, 403 pp.

Brown, G. C., Hughes, D. J. & Esson, J., 1973. New X.R.F. data retrieval techniques and their application to U.S.G.S. standard rocks. *Chemical Geology* **11**, 223–229.

Cartwright, I., Valley, J. W. & Hazelwood, A. M., 1993. Resetting of oxybarometers and oxygen isotope ratios in granulite facies orthogneisses during cooling and shearing. Adirondack Mountains, New York. *Contributions to Mineralogy and Petrology* **113**, 208–225.

Chappell, B. W. & Stephens, W. E., 1988. Origin of infracrustal (I) type granite magmas. *Transactions of the Royal Society of Edinburgh Earth Science* **79**, 71–86.

Chappell, B. W. & White, A. J. R., 1974. Two constrasting granite types. *Pacific Geology* **8**, 173–174.

Christensen, N. I., 1982. Seismic velocities. In: Carmichael, R. S. (ed.) *Handbook of Physical Properties of Rocks 2*. Boca Raton, FL: CRC Press, 228 pp.

Clayton, R. N. & Mayeda, T. K., 1963. The use of bromine pentafluoride in the extraction of oxygen from oxides and silicates for isotopic analysis. *Geochimica et Cosmochimica Acta* **27**, 43–52.

Cobbing, E. J., 1985. The tectonic setting of the Peruvian Andes. In: Pitcher, W. S., Atherton, M. P., Cobbing, E. J. & Beckinsale, R. D. (eds) *Magmatism at a Plate Edge: the Peruvian Andes*. Glasgow: Blackie Halstead Press, pp. 167–176.

Cobbing, E. J., Pitcher, W. S., Wilson, J. J., Baldcock, J. W., Taylor, W. P., McCourt, W. J. & Snelling, N. J., 1981. The geology of the western Cordillera of Northern Peru. *Overseas Memoir of Institute of Geological Sciences* **5**, 143 pp.

Couch, R., Whitsett, R., Huehn, B. & Bricêno-Guarupe, L., 1981. Structures of the continental margin in Peru and Chile. In: Kulm, L. D., Dymond, D., Dasch, E. & Hussong, D. M. (eds) *Nazca Plate: Crustal Formation and Andean Convergence. Geological Society of America, Memoir* **154**, 703–726.

Davidson, J. P., Harmon, R. S. & Worner, G., 1991. The source of central Andean magmas; some considerations. In: Harmon, R. S. & Rapela, C. W. (eds) *Andean Magmatism and its Tectonic Setting. Geological Society of America, Special Paper* **265**, 233–257.

Davies, J. H. & Bickle, M. J., 1991. A physical model for the volume and composition of melt produced by hydrous fluxing above subduction zones. *Philosophical Transactions of the Royal Society of London* **335**, 355–364.

Davies, J. H. & Stevenson, D. J., 1992. Physical model of source regions of subduction zone volcanics. *Journal of Geophysical Research* **97**, 2037–2070.

Defant, M. J. & Drummond, M. S., 1990. Derivation of some modern arc magmas by melting of young subducting lithosphere. *Nature* **347**, 662–665.

Dewey, J. F., 1988. Extensional collapse of orogens. *Tectonics* **7**, 1123–1139.

Drummond, M. S. & Defant, M. J., 1990. A model for trondhjemite–tonalite–dacite genesis and crustal growth via slab melting. Archean to modern comparisons. *Journal of Geophysical Research* **95**, 21503–21521.

Duffield, J. & Gilmore, G. R., 1979. An optimum method for the determination of REE by N.A.A. *Journal of Radioanalytical Chemistry* **48**, 135–145.

Egeler, C. G. & De Booy, T., 1956. Geology and petrology of part of the southern Cordillera Blanca, Peru. *Verhandelingen van het Koninklijk Nederlandsch Geologisch-Mijnbouwkundig Genootshap, Geologische Serie* **17**, 1–86.

Fukao, Y., Yamamoto, A. & Kong, M., 1989. Gravity anomaly across the Peruvian Andes. *Journal of Geophysical Research* **94**, 3867–3890.

Furlong, K. & Fountain, D. M., 1986. Continental crustal underplating: thermal considerations and seismic–petrological considerations. *Journal of Physical Research* **91**, 8285–8294.

Hanson, G. N., 1980. Rare earth elements in petrogenetic studies of igneous systems. *Annual Review of Earth and Planetary Sciences* **8**, 371–406.

Herzberg, C. T., Fyfe, W. S. & Carr, M. J., 1983. Density contrasts on the formation of the continental Moho and crust. *Contributions to Mineralogy and Petrology* **84**, 1–5.

Hildreth, W. & Moorbath, S., 1988. Crustal contributions to arc magmatism in the Andes of central Chile. *Contributions to Mineralogy and Petrology* **98**, 455–489.

Hildreth, W., Christiansen, R. L. & O'Neil, J. R., 1984. Catastrophic isotopic modification of rhyolite magma at times of caldera subsidence, Yellowstone plateau volcanic field. *Journal of Geophysical Research* **89**, 8339–8369.

Jahn, B. M., Vidal, P. & Kroner, A., 1984. Multichronometric ages and origin of Archean tonalitic gneisses in Finnish Lapland: a case for long crustal residence time. *Contributions to Mineralogy and Petrology* **86**, 389–408.

James, D. E., 1971. Andean crustal and upper mantle structure. *Journal of Geophysical Research* **76**, 3246–3271.

Kay, R. W. & Kay, S. M., 1991. Creation and destruction of lower continental crust. *Geologische Rundschau* **80**, 259–278.

Kono, M., Fukao, Y. & Yamamoto, A., 1989. Mountain building in the central Andes. *Journal of Geophysical Research* **94**, 3891–3905.

Lameyre, J. & Bowden, P., 1982. Plutonic rock type series: discrimination of various granitoid series and related rocks. *Journal of Volcanology and Geothermal Research* **14**, 169–186.

Lopez-Escobar, L., Frey, F. A. & Oyarzun, J., 1979. Geochemical characteristics of central Chile (33–34°S) granitoids. *Contributions to Mineralogy and Petrology* **70**, 439–450.

Martin, H., 1986. Effect of steeper Archean geothermal gradient on geochemistry of subduction zone magmas. *Geology* **14**, 753–756.

Martin, J., 1987. Petrogenesis of Archean trondhjemites, tonalites and granodiorites from eastern Finland: major and trace element geochemistry. *Journal of Petrology* **28**, 921–953.

Mason, G. H., 1985. The mineralogy and textures of the Coastal Batholith, Peru. In: Pitcher, W. S., Atherton, M. P., Cobbing, E. J. & Beckinsale, R. D. (eds) *Magmatism at a Plate Edge: the Peruvian Andes*. Glasgow: Blackie Halstead Press, pp. 156–166.

McCourt, W. J., 1978. The geochemistry and petrogenesis of the Coastal Batholith of Peru, Lima segment. Ph.D. Thesis, University of Liverpool.

McDonough, W. F. & Frey, F. A., 1989. Rare earth elements in upper mantle rocks. In: Lipman, B. R. & McKay, G. A. (eds) Geochemistry and mineralogy of rare earth elements. *Mineralogical Society of America, Reviews in Mineralogy* **21**, 99–140.

McMillan, N. J., Davidson, J. P., Warner, G., Harmon, R. S., Moorbath, S. & Lopez-Escobar, L., 1993. Influence of crustal thickening on arc magmatism: Navados de Payachata volcanic region, northern Chile. *Geology* **21**, 467–470.

Mégard, F., 1989. The evolution of the Pacific ocean margin in South America, north of Africa elbow (18°S). In: Ben-Avraham

Z. (ed.) *The Evolution of the Pacific Ocean Margins. Oxford Monograph on Geology and Geophysics 8.* Oxford: Oxford University Press, pp. 208–230.

Mégard, F. & Philip, H., 1976. Plio-Quaternary tecto-magmatic zonation and plate tectonics in the central Andes. *Earth and Planetary Science Letters* **33,** 231–238.

Miller, C. F. & Bradfish, L. J., 1980. An inner belt of muscovite bearing plutons. *Geology* **8,** 412–416.

Miller, C. F., Stoddard, E. F., Bradfish, L. J. & Dollase, W. A., 1981. Composition of plutonic muscovite: genetic implications. *Canadian Mineralogist* **19,** 25–34.

Miller, N. & Harris, N., 1989. Evolution of continental crust in the central Andes; constraints from Nd isotope systematics. *Geology* **17,** 615–617.

Mukasa, S. B., 1984. Comparative Pb isotope systematics in batholithic rocks from the Coastal, San Nicholas and Cordillera Blanca Batholiths, Peru. Ph.D. Thesis, University of California, Santa Barbara.

Mukasa, B. K. & Tilton, G. R., 1984. Lead isotope systematics in batholithic rocks of the western and coastal Cordilleras, Peru. In: Harmon, R. S. & Barreiro, B. A. (eds) *Andean Magmatism: Chemical and Isotopic Constraints.* Nantwich, UK: Shiva, pp. 180–189.

Nash, W. P. & Crecraft, H. R., 1985. Partition coefficients for trace elements in silicic magmas. *Geochimica et Cosmochimica Acta* **49,** 2309–2322.

Nelson, K. D., 1992. Are crustal thickness variations in old mountain belts like the Appalachians a consequence of lithospheric delamination? *Geology* **20,** 498–502.

Norrish, K. & Hutton, V. T., 1969. An accurate X-ray spectrographic method for the analysis of a whole range of geological samples. *Geochimica et Cosmochimica Acta* **33,** 431–453.

Ocola, L. C. & Meyer, R. P., 1972. Crustal low velocity zones under the Peru–Bolivia Altiplano. *Geophysical Journal of the Royal Astronomical Society* **30,** 199–209.

O'Connor, J. T., 1965. A classification for quartz-rich igneous rocks based on feldspar ratios. *US Geological Survey, Professional Papers* **525B,** B79–B84.

O'Neil, J. R., 1986. Theoretical and experimental aspects of isotopic fractionation. In: Valley, J. W., Taylor, H. P. & O'Neil, J. R. (eds) *Stable Isotopes in High Temperature Geochemical Processes. Mineralogical Society of America, Reviews in Mineralogy* **16,** 1–40.

Parada, M. A., 1990. Granitoid plutonism in central Chile and its geodynamic implications: a review. In: Kay, S. M. & Rapala, C. W. (eds) *Plutonism from Antarctica to Alaska. Geological Society of America, Special Paper* **241,** 51–66.

Peacock, S. M., 1991. Numerical simulation of subduction zone pressure–temperature–timepaths: constraints on fluid production and arc magmatism. *Philosophical Transactions of the Royal Society of London* **335,** 341–353.

Peacock, S. M., 1993. Large scale hydration of the lithosphere above subducting slabs. *Chemical Geology* **108,** 49–59.

Peacock, S. M., Rushmer, T. & Thompson, A. B., 1994. Partial melting of subducting oceanic crust. *Earth and Planetary Science Letters* **121,** 227–244.

Petford, N., 1990. The relation between deformation, granite source type and crustal growth: Peru. Ph.D. Thesis, University of Liverpool.

Petford, N. & Atherton, M. P., 1992. Granitoid emplacement and deformation along a major crustal lineament: the Cordillera Blanca, Peru. *Tectonophysics* **205,** 171–185.

Petford, N., Atherton, M. P. & Halliday, A. N., 1996. Rapid magma production rates, underplating and remelting in the Andes: isotopic evidence from northern–central Peru (9–11°S). *Journal of South American Earth Sciences* **9,** 69–78.

Pilger, R. H., 1984. Cenozoic plate kinematics, subduction and magmatism: South American Andes. *Journal of the Geological Society of London* **41,** 793–802.

Pitcher, W. S., 1983. Granite type and tectonic environment. In: Hsui, K. (ed.) *Mountain Building Processes.* London: Academic Press, pp. 19–40.

Pitcher, W. S., Atherton, M. P., Cobbing, E. J. & Beckinsale, R. D., 1985. *Magmatism at a Plate Edge: the Peruvian Andes.* Glasgow: Blackie Halstead Press, 329 pp.

Rapp, R. P. & Watson, E. B., 1995. Dehydration melting of metabasalt at 8–32 kbar: implications for continental growth and crust–mantle recycling. *Journal of Petrology* **36,** 891–931.

Rapp, R. P., Watson, E. B. & Miller, C. F., 1991. Partial melting of amphibolite/eclogite and the origin of Archean trondhjemites and tonalites. *Precambrian Research* **51,** 1–25.

Rushmer, T., 1993. Experimental high pressure granulites: some applications to natural mafic xenolith suites and Archean granulite terrranes. *Geology* **21,** 411–414.

Schmitz, M., 1994. A balanced model of the southern central Andes. *Tectonics* **13,** 484–492.

Schmucker, U., 1969. Conductivity anomalies with special reference to the Andes. In: Runcorn, S. K. (ed.) *The Application of Modern Physics to the Earth and Planetary Interiors.* New York: Wiley Interscience, pp. 125–138.

Sebrier, M., Mercier, J. L., Marchare, J., Bonnot, D., Cabarez, J. & Blanc, J. L., 1988. The state of stress in an over-riding plate situated above a flat slab: the Andes of central Peru. *Tectonics* **7,** 895–928.

Sen, C. & Dunn, T., 1994. Dehydration melting of basaltic composition amphibolite at 1·5 and 2·0 GPa: implications for the origin of adakites. *Contributions to Mineralogy and Petrology* **117,** 394–409.

Spulber, S. D. & Rutherford, M. J., 1983. The origin of rhyolite and plagiogranite in oceanic crust: an experimental study. *Journal of Petrology* **24,** 1–25.

Steinmann, G., 1910. Gebirgsbildung und Massengestaine in der Kordillere Sud Amerikas. *Geologische Rundschau* **1,** 13–35.

Stern, C. R., Futa, K. & Muchlenbacks, K., 1984. Isotopic and trace element data for orogenic andesites from the Austral Andes. In: Harmon, R. S. & Barreiro, B. A. (eds) *Andean Magmatism, Chemical and Isotopic Constraints.* Nantwich, UK: Shiva, pp. 31–46.

Stewart, J. W., Evernden, J. F. & Snelling, N. J., 1974. Age determinations from Andean Peru: a reconnaissance survey. *Geological Society of America Bulletin* **85,** 1107–1116.

Suarez, G., Molnar, P. & Burchfiel, B. C., 1983. Seismicity, fault plane solutions, depth of faulting and active tectonics of the central Andes. *Journal of Geophysical Research* **88,** 403–428.

Tatsumi, Y., 1989. Migration of fluid phases and genesis of basalt magmas in subduction zones. *Journal of Geophysical Research* **94,** 4697–4707.

Taylor, H. P., 1986. Igneous rocks II. Isotopic case studies of circum-Pacific magmatism. In: Valley, J. W., Taylor, H. P. & O'Neil, J. R. (eds) *Stable Isotopes in High Temperature Geochemical Processes. Mineralogical Society of America, Reviews in Mineralogy* **16,** 273–317.

Thorpe, R. S., Francis, P. W. & Harmon, R. S., 1981. Andean crustal growth. *Philosophical Transactions of the Royal Society of London, Series A* **301,** 305–320.

Tilton, G. R. & Barreiro, B. A., 1980. Origin of lead in Andean calc-alkaline lavas, southern Peru. *Science* **210,** 1245–1247.

Toft, P. B., Hills, D. V. & Haggerty, S. E., 1989. Crustal evolution and the granulite to eclogite transition in xenoliths from kimberlites in the west African craton. *Tectonophysics* **161,** 213–231.

Uyeda, S. & Watanabe, T., 1970. Preliminary report of terrestrial heat flow study in the South American continent; distribution of geothermal gradients. *Tectonophysics* **10,** 235–242.

Van de Laan, S. R. & Wyllie, P. J., 1992. Constraints on Archean trondhjemite genesis. *Journal of Geology* **100,** 57–68.

Wilson, C. D. V., 1985. The deep structure of the central Andes and some geophysical constraints. In: Pitcher, W. S., Atherton, M. P., Cobbing, E. J. & Beckinsale, R. D. (eds) *Magmatism at a Plate Edge: the Peruvian Andes*. Glasgow: Blackie Halstead Press, pp. 13–18.

Wilson, J. J. & Garayar, J., 1967. Geología de los cuadrángulos de Mollenbamba. Tayabamba, Huaylas, Pomabamba, Carhuaz y Huari. *Servicio de Geologia y Mineria Peru, Boletin* **22,** 95 pp.

Wilson, M., 1989. *Igneous Petrogenesis*. London: Unwin Hyman, 466 pp.

Wortel, M. J. R., 1984. Spatial and temporal variations in the Andean subduction zone. *Journal of the Geological Society of London* **141,** 783–791.

RECEIVED OCTOBER 26, 1994
REVISED TYPESCRIPT ACCEPTED JUNE 21, 1996